CHAPTER 24

Himalayan glaciers (India, Bhutan, Nepal): Satellite observations of thinning and retreat

Adina E. Racoviteanu, Yves Arnaud, I.M. Baghuna, Samjwal R. Bajracharya, Etienne Berthier, Rakesh Bhambri, Tobias Bolch, Martin Byrne, Ravinder K. Chaujar, Regula Frauenfelder, Andreas Kääb, Ulrich Kamp, Jeffrey S. Kargel, Anil V. Kulkarni, Gregory J. Leonard, Pradeep K. Mool, and I. Sossna

ABSTRACT

This chapter summarizes the current state of remote sensing of glaciers in the India, Nepal, and Bhutan regions of the Himalaya, and focuses on new methods for assessing glacier change. Glaciers in these Himalaya regions exhibit complex patterns of changes due to the unique and variable climatic, topographic, and glaciological parameters present in this region. The theoretical understanding of glaciers in the Himalaya is limited by lack of sufficient observations due to terrain breadth and complexity, severe weather conditions, logistic difficulties, and geopolitics. Mapping and assessing these glaciers with satellite imagery is also challenging due to inherent sensor limitations and information extraction issues. Thus, we still lack a complete understanding of the magnitude of feedbacks, and in some places even their sign, between climate changes and glacier response in this region. In this chapter we present the current status of glaciers in various climatic regimes of the Himalaya, ranging from the monsoon-influenced regions of the central–eastern Himalaya (Nepal, Garhwal, Sikkim, and Bhutan) through the monsoon transition zone of Himachal Pradesh (India), to the dry areas of Ladakh (western Himalaya). The case studies presented here illustrate the use of remote sensing and elevation data coupled with glacier-mapping techniques for glacier area and elevation change detection and ice flow modeling in the context of the Himalaya.

24.1 OVERVIEW

Glaciers constitute a significant component of the hydrologic regime of the Himalaya in terms of their importance for regional water supply for irrigation, hydropower generation, and consumption. There are concerns about the potential social and economic impacts of glacier shrinkage in the last decade (Dyurgerov 2002 [2005]; Barnett et al. 2005; Barry 2006). Of particular concern is the impact of glacier changes on regional water supplies (Barnett et al. 2005, Kaser et al. 2010), their contribution to sea level rise (Kaser et al. 2006), and increased natural hazards such as outburst floods from moraine-dammed lakes (Richardson and Reynolds 2000, Mool et al. 2002a, Bajracharya et al. 2007, 2008, Bolch et al. 2008a). Glacier shrinking contributes to the fast growth of glacial lakes, with some of these being converted to moraine-dammed lakes (Hambrey et al. 2008). These lakes occasionally breach the moraine dam (Watanabe et al. 1995), in some cases resulting in downstream valleys suffering catastrophic impacts. Many studies have reported high rates of wastage of the Himalayan glaciers in recent decades (Fujita et al. 2001, Kulkarni and Bahuguna 2002, Karma et al. 2003, Fujita

J. S. Kargel et al. (eds.), *Global Land Ice Measurements from Space*, Springer Praxis Books,
DOI: 10.1007/978-3-540-79818-7_24,

and Nuimura 2011, Kargel et al. 2011, Scherler et al. 2011, Azam et al. 2012, Yao et al. 2012), although in individual studies such trends are commonly based on one to a few unrepresentative sites, and even taken together they do not capture the entire complexity of glacier response to climate change in the Himalaya. Nevertheless, the body of evidence about the impacts of glacier changes is growing and clearly indicates some spatial patterns, which we shall further describe and exemplify with case studies.

Furthermore, claims that Himalayan glaciers are melting at higher rates than glaciers in other mountain ranges and may even disappear by 2035, as reported by IPCC (2007) and WWF (2005), were found to be erroneous and linked to a typographical mistake and a sequence of other errors and misjudgments (Cogley et al. 2010). It has been shown that Himalayan glaciers are primarily thinning and many are retreating, but the overall negative mass balance of the Himalaya proper (as defined in the next section) is within the typical range of alpine glaciers worldwide (Bolch et al. 2012). Glaciers in the Karakoram are complex and possibly show a slight mass gain on average since 1999; however, locally in the Karakoram some glaciers are clearly growing (Hewitt 2011, Bolch et al. 2012, Gardelle et al. 2012a, Yao et al. 2012). This may partly balance shrinking ice masses in the rest of the Himalaya, reported in various other studies (Bhambri et al. 2011, Fujita and Nuimura 2011, Bolch et al. 2012), such that the net mass balance of the entire Karakoram Himalaya region may be only slightly negative.

There is a complex pattern of glacier changes across the Himalaya (Kargel et al. 2011). Although some theoretical understanding of climate underpinnings is starting to emerge (Fujita et al. 2011, Scherler et al. 2011, Bolch et al. 2012), we still lack a complete fundamental understanding of the magnitude of feedbacks, and in some places even their sign, between climate change and glacier response in this region. The numerous climatic, topographic, and glaciological parameters that govern glacier fluctuations are not well understood. Furthermore, particulate soot and other pollutants are thought to have substantial impacts on the mass balance of glaciers in High Asia (Lau et al. 2010, Ming et al. 2012). Theoretical understanding of glaciers in the Himalaya is hampered by the lack of sufficient observations due to terrain breadth and complexity, severe weather conditions, logistic difficulties, and geopolitics. Mapping and assessing Himalayan glaciers with satellite imagery is also notoriously difficult due to inherent sensor limitations and information extraction issues (Bishop et al. 2001, Kargel et al. 2005). For example, the use of remote sensing for glaciological applications is limited by spatiotemporal spectral variations, frequent cloud cover, and saturation due to dynamic glacier surfaces and sensor gain settings. This includes mapping small glaciers and debris-covered glaciers, and assessing terminus fluctuations given temporal coverage limitations. Remote-sensing glacier assessments in monsoon-influenced parts of the Himalaya are further limited by the persistence of seasonal snow, making satellite image acquisition challenging in this area. Glacier elevation changes and ice velocity estimates are constrained by systematic biases in digital elevation models such as SRTM data (Berthier et al. 2006, Gardelle et al. 2012b). Nevertheless, new approaches to information extraction have been developed, and remote sensing of glaciers in the Himalaya is becoming increasingly useful for quantitative assessment of glacier parameters. Among these, false-color composites and band ratios from visible and near-infrared satellite images have been used successfully to map various glacial features such as glacier boundaries, accumulation areas, ablation areas, equilibrium lines and moraine-dammed lakes. These features are extracted using differences in the spectral reflectance of glacial and nonglacial features.

This chapter summarizes the current state of remote sensing of glaciers in the India, Nepal, and Bhutan regions of the Himalaya. Specifically, we present glacier changes in various climatic regimes of the Himalaya, ranging from the monsoon-influenced regions of the central–eastern Himalaya (Nepal Himalaya, Garhwal Himalaya, Sikkim, and Bhutan) to the monsoon transition zone of Himachal Pradesh in the western Himalaya (India) and the dry areas of Ladakh. The case studies presented here illustrate the use of remote sensing and elevation data coupled with glacier-mapping techniques for change detection, glacier runoff, and ice flow modeling in the context of the Himalaya.

24.2 REGIONAL CONTEXT

24.2.1 Geographic, geologic, and topographic setting

Various terms are used to refer to the Himalayan ranges: some of the earlier studies (Mason 1954)

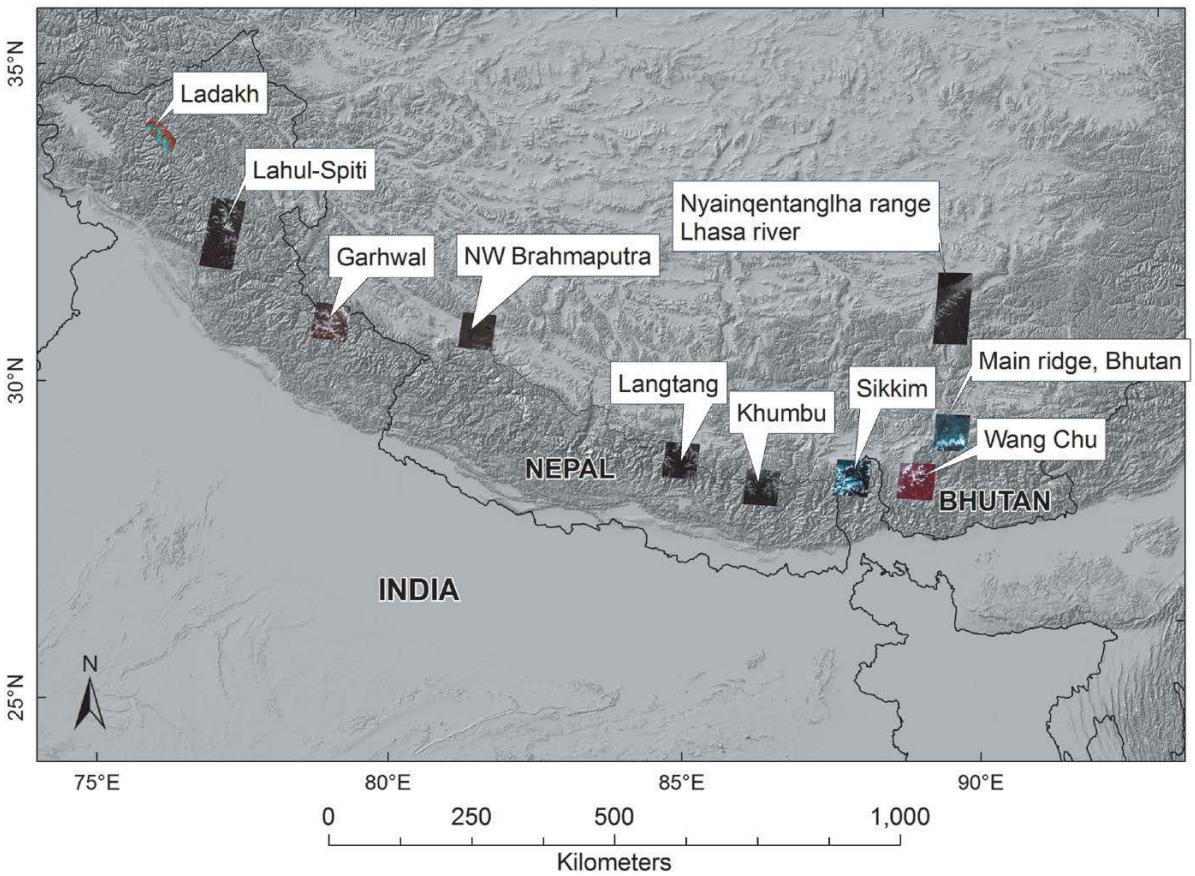

Figure 24.1. Study area showing the regions analyzed in this chapter, covering the Himalaya from east to west. The study regions are snapshots of ASTER scenes shown on topography from the SRTM DEM.

split the Himalaya into subdivisions: western Himalaya (Nanga Parbat in the Karakoram of Pakistan, Himachal Pradesh in India), central Himalaya (Garhwal, Nepal) and eastern Himalaya (Sikkim and Bhutan). Mayewski et al. (1979, 1980) distinguish between Himalaya (Everest–Kanchenjunga region, Garhwal, Himachal, and Nanga Parbat) and trans-Himalaya (Karakoram, Batura-Muztagh, north Karakoram and Khunjerab-Ghujerab). Ren et al. (2007) refer to the "Greater Himalaya" as the region spanning 25–45°N to 70–105°E, which includes the Qinghai-Xizang Plateau and the Tien Shan range. In this contribution, we define the Himalaya as the region extending in a southeast–northwest direction between ~27–32° latitude and 77–92° longitude, south of the Tibetan Plateau (Fig. 24.1). In this chapter, we adopt Mayewski's definition, but exclude the Tibetan (Chinese) side of the Himalayan range (covered in Chapter 25 of this book by Liu et al.), and the Hindu Kush and Karakoram ranges.

Geologically, the Himalaya is a product of long-term and still active plate-tectonic collision resulting in numerous suture zones, intrusive granitoid bodies, and stacks of south-vergent thrust sheets and nappe folds. The Himalaya consists of a broad sweep of multiple ranges, with few sharp topographic boundaries, and is generally considered separate from the Pamir and Hindu Kush, which extend along different structural strike directions from Pakistan into Afghanistan and Tajikistan. The Himalaya range is wider on the west (~400 km), and narrower on the east (~50 km). Topography is more rugged in the western part of the range as a result of scale-dependent erosion processes, which produce complex relief and morphology patterns (Bishop et al. 2002). The southern slopes of the Himalaya have steep relief, with large undulations and elevations ranging from ~2,000 m in the foothills to the highest summit, Mt. Everest (8,848 m). The Himalaya are host to some of the largest glaciers outside the polar regions. Many are

characterized by the presence of thick debris cover at their tongues, due to rockfall debris originating from the steep sides falling onto accumulation zones, with subsequent transport downglacier to the ablation area (Singh 2000, Takeuchi et al. 2000). This creates some very long valley glaciers such as Bara Shigri (28 km), Gangotri (30 km), Zemu (26 km), Milam (19 km), and Kedarnath (14.5 km) in the Indian Himalaya (Shen, 2004).

24.2.2 Climate dynamics and glacier regimes

The climate of the Himalaya is dominated by the South Asian summer monsoon (commonly called the Indian monsoon) circulation system, often described as a gigantic sea breeze. Gadgil (2003) explained the South Asian monsoon as the seasonal migration of the Intertropical Convergence Zone, which is the ascending flow that separates the northern and southern cells of idealized Hadley (equator to poles) circulation. These two climatic mechanisms (the sea breeze and the Hadley cell circulation) both appear to be important and can interplay with each other; thus, both may participate in driving the monsoon. Mid-tropospheric heating over the Tibetan Plateau during the summer causes the inflow of moist air from the Bay of Bengal to the continent (Yanai et al. 1992, Benn and Owen 1998). The Himalaya and Tibetan Plateau (HTP) acts as a barrier to monsoon winds, inducing maximum precipitation on the south slopes of the Himalaya during the summer (June to September) (Gautam et al. 2009). Convection over the HTP region during the monsoon season releases latent heat, thus sustaining the monsoon (Barros and Lang 2003, Bhatt and Nakamura 2005). In the winter, westerly winds occasionally bring heavy snowstorms to the western ranges of the Indian Himalaya, due to moisture originating from the Mediterranean, Black, and Caspian Seas (Higuchi et al. 1992, Benn and Evans 1998). There is an east–west gradient in monsoon intensity, with higher precipitation amounts in the central Himalaya (Nepal and Garhwal), and lower precipitation amounts in Lahaul-Spiti and Ladakh. Large amounts of monsoon rainfall (300–400 cm yr^{-1}) occur on the south slopes of the Himalaya (Shrestha 2000), posing concerns for erosion and flooding in these areas (Bookhagen and Burbank 2006).

Glacier regimes vary across the Himalaya depending on their location with respect to two large-scale circulation patterns: the Asian monsoon and the westerlies. Central–eastern Himalayan glaciers (Nepal and Garhwal) are of summer accumulation type, with maximum snowfall and ablation, and most accumulation, occurring in the summer (Ageta and Higuchi 1984, Dobhal et al. 2008). Glaciers in the western regions (Lahaul-Spiti and Ladakh) experience maximum precipitation in the winter, and are considered to be of the winter accumulation type (Benn and Owen 1998). In general, accumulation on Himalayan glaciers occurs mostly by snowfall, blowing snow, and avalanches from steep mountain slopes (Benn and Owen 1998).

There is concern about climate change in the Himalaya in past and coming centuries, and their consequences on glacier mass balance. Analysis of climate records from station data show increasing mean annual temperatures in the northwestern Himalaya (Bhutiyani et al. 2007, 2010, Shekhar et al. 2010) and the central and eastern Himalaya (Shrestha et al. 1999). Microwave satellite measurements of tropospheric temperature (1979–2007) also indicate accelerated annual mean warming over the Himalayan region (reported as $0.21 \pm 0.08^{\circ}C$/decade), with a maximum warming over the western Himalaya ($0.26 \pm 0.09^{\circ}C$/decade) (Gautam et al. 2010). Surface flux and aerosol measurements point to an increase in radiative heating from dust aerosol absorption over the Indo-Gangetic Plain in the pre-monsoon period, which may explain accelerated seasonal warming (Gautam et al. 2010). The increase in temperature appears to be concomitant with decreasing trends in monsoon precipitation (Bhutiyani et al. 2010), and a reduction in total seasonal snowfall (Dimri and Kumar 2008, Shekhar et al. 2010) for the same period. These increasing trends in temperature in the central and eastern Himalaya are consistent with widespread glacier shrinkage in the last decades, reported in various studies (Yamada et al. 1992, Fujita et al. 1997, 2001, Kadota et al. 2000, Kulkarni and Bahuguna 2002, Bolch et al. 2008b, 2012, Bhambri et al. 2011). In contrast, the Karakoram range to the west of the Himalaya has experienced a decreasing trend in maximum and minimum temperatures of 1.6 and $3^{\circ}C$, respectively (Shekhar et al. 2010), along with an increase in winter precipitation (Fowler and Archer 2006) in the last decades. These trends seem consistent with lower rates of retreat of glaciers and stable termini, or alternating retreat and advance reported from some glaciers in the Karakoram and the northwest Himalaya (Schmidt and Nusser 2009, Hewitt 2011). Rapid thickening trends have also been reported in

this area; however, these are anomalies associated with topographic control on mass balance, mainly an elevation effect rather than climate-induced change (Hewitt 2005). At least for the first decade of the 21st century, a slight gain of mass for a large subset (over 5,500 km^2) of Karakoram glaciers has been recently confirmed (Gardelle et al. 2012a). In summary, further work is needed to estimate east–west trends in precipitation patterns and their effect on glacier fluctuations, the magnitude of ice velocities, and regional mass balance in various areas of the Himalaya.

24.2.3 Previous glacier mapping and observations

Long-term assessments of glacier change in the Himalaya have been limited mostly to direct observations of glacier termini. Field-based glacier mass balance studies are scarce, limited to a few glaciers, and most often not in the public domain. Long-term mass balance records and assessments of spatial variations of glaciological parameters and change over the Himalaya are still missing from global records (Dyurgerov and Meier 2005, Kaser et al. 2006). Some of the available mass balance measurements are provided in Cogley et al. (2009) and Raina (2009). Among the main challenges in glacier change detection in the Himalaya are: (1) the lack of comprehensive accurate baseline glacier inventories to use as a basis for comparison with new glacier data from remote sensing; (2) recent Indian glacier inventories, such as those based on Indian Remote Sensing (IRS) sensors series are not in the public domain (e.g., Kulkarni and Buch 1991, Kulkarni 1992, Bahuguna et al. 2001, Krishna 2005); and (3) the Indian glacier inventory based on Survey of India maps at 1:50,000 scale, published by the Geologic Survey of India (GSI) (Sangewar and Shukla 1999) or the Glacier Atlas of India (Raina and Srivastava 2008) neither of which are available in digital form. For India, the earliest glacier maps are available from topographic surveys conducted by expeditions in the mid-19th century in India (Mason 1954). Some of the earlier glacier inventories for the Indian Himalaya include Sah et al. (2005) and Bhagat et al. (2004). However, the use of these inventories is often limited due to georeferencing problems associated with old topographic maps and satellite imagery, which can be of the order of a few hundred meters. Some of these problems are discussed in Vohra (1980). For a more detailed literature review of Indian glacier inventories and their limitations, the reader is directed to a recent review by Bhambri and Bolch (2009). For Nepal, a glacier inventory has been compiled on the basis of topographic maps from the 1970s and 1980s (Mool et al. 2002). The eastern part of the Nepal Himalaya has been mapped on the basis of field observations and aerial photos (Higuchi et al. 1980) as well as Schneider's 1:50,000 topographic maps (Müller 1970). A glacier inventory of Bhutan has been compiled by Mool et al. (2002); some glacier data have also been published by Karma et al. (2003). A new glacier inventory of the Hindu Kush Himalayan region including Afghanistan, Bhutan, India, Myanmar, Nepal, Pakistan and part of China has been recently completed based on ~2005 Landsat data (Bajracharya and Shrestha 2011). Recently, results of a large satellite image-based effort to re-inventory glaciers across the whole Himalaya–Karakorum region has been published in preliminary form (Bajracharya et al. 2011).

24.3 CASE STUDIES AND SPECIFIC TOPICS

In this section we summarize changes in glacier area, thickness, and velocities across the Himalaya based on case studies conducted across the mountain range. The case studies are organized by region, proceeding from east to west, which is also roughly in accordance with weakening monsoon influences. We present standardized glacier inventory techniques based on remote sensing and GIS (e.g., semi-automated band ratio techniques), as well as more innovative techniques such as surface reflectance changes. Change detection is conducted at the decadal scale, spanning the period of observations from satellite monitoring.

24.3.1 Sikkim Himalaya: glacier area change, 1960–2000

24.3.1.1 Introduction

This study relies on remote-sensing data from ASTER, Landsat ETM+, Corona, QuickBird, and WorldView-2 sensors to investigate spatial patterns of glacier parameters in Sikkim, which is located in the eastern Himalaya (27°04′52″N to 28°08′26″N and 88°00′57″E to 88°55′50″E). Specifically, we present: (1) a new geospatial glacier inventory based on 2000 Landsat and ASTER imagery and (2) glacier area and elevation changes

in the last four decades based on multitemporal data. The Sikkim Himalaya is located in eastern India, between Nepal and Bhutan, and is subject to a monsoon-dominated climate (Fig. 24.1). Elevations range from 300 m in the eastern parts to 8,598 m at the summit of Mt. Kanchenjunga (the third largest mountain in the Himalaya). Terrain is steep and rugged, and many glacier tongues are covered with debris in their ablation zones. The glacier inventory compiled by the Geological Survey of India, based on topographic maps from the 1960s–1970s, lists 449 glaciers covering an area of 705.54 km^2 (Shanker 1999, Sangewar and Shukla 2009). Mool et al. (2002) reported 285 glaciers covering an area of 576.4 km^2 on the basis of 2000 Landsat imagery. There is concern about the growth of potentially dangerous supraglacial lakes in this area (Mool et al. 2002).

24.3.1.2 Methods

The Swiss Foundation for Alpine Research topographic map at 1:150,000 scale, compiled from Survey of India maps dating from the 1960s to 1970s, was used as the baseline dataset for this study. Most Survey of India maps generally date from 1962, but the exact date of each quadrant is not known with certainty. The availability of original large-scale Indian topographic maps at this scale is restricted within 100 km of the Indian border (Srikantia 2000, *Survey of India* 2005). Therefore, we assumed a reference date for this topographic map of the 1960s or thereabouts, with an error term of about one decade. The remote-sensing data used here included: ASTER, Landsat ETM+, Corona KH4, QuickBird and WorldView-2 (Table 24.1). A Landsat ETM+ scene from December 2000 and six orthorectified ASTER scenes (2000 to 2005) were used to compile an updated inventory, with a reference date here of the 2000s or thereabouts. The Landsat scene covered a larger spatial domain including Nepal, Sikkim, and parts of China and Bhutan; the ASTER scenes covered mainly Sikkim. Three Corona KH4 scenes (from 1962) were obtained from the U.S. Geological Survey EROS Data Center (USGS-EROS 1996). Nominal ground resolution for the KH4 mission was 7.62 m (Dashora et al. 2007). However, optimal pixel size calculated using the scale of the photos and the scan resolution was 2 m. The Corona scenes were orthorectified using ground control points (GCPs) extracted from the panchromatic band of the Landsat scene (15 m spatial resolution), using the bundle block adjustment procedure in ERDAS Imagine's Leica Photogrammetric Suite (LPS). Elevations were extracted from the void-filled Shuttle Radar Topography Mission (SRTM) DEM (version CGIAR-CSI 2004). All images were acquired at the end of the ablation season (October–November), were mostly cloud free, and showed good contrast over snow and ice.

Baseline glacier outlines (~1960s) were delineated manually from the topographic map and the Corona 1962 panchromatic image. New glacier outlines (2000) were mapped onto Landsat ETM+ imagery using standardized semiautomated methods described in detail in Racoviteanu et al. (2009). The normalized difference snow index (NDSI) algorithm (Hall et al. 1995), with a threshold of 0.7 ($NDSI > 0.7 = snow/ice$) and a 3×3 median filter was used to obtain a map of clean ice. The Landsat-based outlines were complemented with ASTER images in areas of clouds and shadow, which had to be edited manually. Debris-covered areas were delineated using a decision tree classifier in ENVI, in which we combined surface reflectance, topography, and kinetic surface temperature from ASTER thermal bands (AST08 product) (Racoviteanu et al. 2008, Racoviteanu and Williams 2012). The decision tree eliminates areas that are not "suitable" for the presence of debris cover based on information extracted from the topographic map, such as the presence of clean ice or vegetation. Glacier outlines were validated on the basis of high-resolution imagery from QuickBird (QB) and WorldView-2 (WV2) obtained from Digital Globe. Ice masses were split into individual glaciers using topographic information from the SRTM DEM and the protocol developed by Manley (2008). Glacier parameters such as terminus elevation, median and minimum elevation, and glacier hypsometry (area–altitude distribution) were extracted from glacier outlines and SRTM elevations.

24.3.1.3 Results: glacier area changes

The glacier inventory of the 1960s (or thereabouts) that was based on the Swiss Alpine topographic map yielded 158 glaciers covering a total area of 742 km^2 in Sikkim. The 2000 Landsat glacier inventory yielded 185 glaciers with an area of 568.8 km^2. This amounts to an area loss of 173.3 km^2 between the 1960s and 2000, or an area loss of 23.34% and a loss rate of $0.5 \pm 0.2\%$ yr^{-1} com-

puted as total percentage change divided by the number of years; computed according to the compound interest rate formula, the loss rate is 0.67% yr^{-1} (Fig. 24.2). Error terms are calculated by considering the uncertainty regarding the data source of the baseline dataset as ±10 years. The increased number of glaciers from 1960s to 2000s indicates ice disintegration, as reported for other parts of the Himalaya (Kulkarni et al. 2007, Bhambri et al. 2011). Overall, there were 22 debris-covered glacier tongues covering an area of 72.2 km^2 in 2000, which represents 13.4% of the entire glacierized area. In 2000, glacier size ranged from 0.05 to 105 km^2, with an average size of 4 km^2. Average terminus elevation increased from 3,317 m in the 1960s to 3,993 m in 2000, a rise of +98 m on average. The average median elevation of glaciers (considered here as a rough estimate of equilibrium line altitude, ELA; Benn and Lehmkuhl 2000) increased from 4,301 m in the 1960s to 4,549 m in 2000, or +107 m. The changes in glacier area are smaller than rates of retreat reported for western parts of the Himalaya ($-0.7 \pm 0.2\%$ yr^{-1}; Kulkarni et al. 2007).

We focused on the Zemu subset of glaciers for area change analysis on the basis of the 1962 Corona scene. Glaciers in this area have lost 15% of their total area in the last 40 years ($\sim 0.4 \pm 0.1\%$ yr^{-1}) compared with a loss of $\sim 0.7 \pm 0.2\%$ yr^{-1} in Sikkim as a whole (total percentage change). The smaller rate of change in the Zemu subset region compared with the entire Sikkim is most likely due to the presence of a few large glacier tongues covered extensively with debris such as Zemu, Yalung, and Talung, which cover a large percent of the subset area. These glaciers tend to lose mass by supraglacial melting and melting underneath the debris cover, resulting in thinning rather than retreating, as shown by studies from the eastern Himalaya and beyond (Nakawo et al. 1993, Nakawo and Rana 1999, Kayastha et al. 2000; Singh et al. 2000, Takeuchi et al. 2000, Bolch et al. 2008b, Scherler et al. 2011). Some studies also showed an increase in the amount of debris cover on glacier tongues concomitant with glacier retreat (Iwata et al. 2000, Bolch et al. 2008b). Our results indicate that the debris-covered glaciers in our study area also experience less change in area than clean small glaciers.

24.3.1.4 Summary of findings

In this study we have combined data from various sensors to compile a new glacier inventory for Sikkim in the eastern Himalaya, and to quantify glacier area change in the last four decades. Based on Landsat/ASTER data and an old topographic map, we have determined area loss of $0.7 \pm 0.2\%$ yr^{-1} between the 1960s and early 2000s. Analysis of 1962 Corona imagery in the Zemu Basin points to smaller rates of retreat of about $0.4 \pm 0.1\%$ yr^{-1}, which we attributed to the presence of glacier tongues extensively covered by debris in this area. We also documented a shift in glacier termini to higher elevations and an increase in glacier ELA. Our results were influenced by the accuracy of satellite imagery, including Landsat/ASTER image classification, and the geolocation of Corona imagery. A few surface types were prone to classification errors from Landsat/ASTER: turbid/frozen lakes were classified as snow/ice because their bulk optical properties were very similar in the visible and near-infrared wavelengths (Dozier 1989a, b); glaciers underneath low clouds could not be classified; transient snow outside glaciers and on the glacier surface could not be distinguished; and debris-covered ice was not distinguished by the NDSI algorithm. These areas had to be adjusted manually. Ground horizontal errors associated with the Corona images (~60 m) were quite large, but inevitable due to distortions in the Corona images, as documented elsewhere (Bolch et al. 2008b). The largest errors were concentrated towards the edges of the images, where GCPs were less reliable. In light of this, we estimated that these horizontal errors would not affect our results considerably. Results of the current study show that glacier area change in the eastern Himalaya is within the range of variability of other areas of the Himalaya, and that these glaciers are not retreating faster than other alpine glaciers in the world, perhaps due to the extensive debris cover on glacier tongues.

24.3.2 Khumbu and Garhwal Himalaya: glacier area and thickness changes, 1960s–2000s

24.3.2.1 Introduction

This section presents glacier changes in two study areas in the central/eastern Himalaya: Garhwal Himalaya, part of the Indian state of Uttarakhand along the border of Tibet/China, and the Khumbu and Imja Valleys south of Mt. Everest in the Solu Khumbu district of Nepal (Fig. 24.1). Both areas are influenced by the Indian summer monsoon and

Table 24.1. Summary of satellite imagery and topographic data used in this chapter.

Study area	*Sensor*	*Year*	*Technique*
Sikkim	Topographic map	~1960s	Manual digitization
	Corona KH4	1962	Image segmentation and manual digitization
	Landsat TM	2000	NDSI (TM1 and TM4) with thresholds; decision tree using topograohic and thermal data for debris-covered ice, with manual corrections
	ASTER	2000, 2003, 2005, 2006	Visual complement for on-screen manual corrections of Landsat data
	IKONOS	2006	Visual comparison/validation of Landsat/ASTER inventory
	WorldView-2	2009	Visual comparison/validation of Landsat/ASTER inventory
Garwhal	ASTER	2006	Band ratios with threshold
	Cartosat-1, IKONOS, IRS LISS	2006	Manual digitization
Khumbu	Corona KH4	1962	Manual digitization in panchromatic mode
	ASTER	2001	Band ratios with threshold
	Cartosat-1, IKONOS, IRS LISS	2001	Manual digitization
Everest	Corona KH4	1962	DEM differencing; relative ASTER DEMs from 2001 to 2003 averaged to one DEM
	Corona KH4B	1972	
	ASTER	2001–2003	
	Cartosat-1	2007	

Brahmaputra	Aerial photos	1960s–1970s	—
	Corona	1960s–1970s	Visual checking of the outlines from aerial photography
	Landsat TM	~2000	Band ratio TM4/5
Wang Chu Basin	Corona KH4B	1974	Manual digitization
	Landsat	2000	Manual digitization
Lunana	ASTER	January 2001–November 2001, October 2002	Horizontal displacements of glaciers (image correlation software, CIAS)
Ladakh	ASTER, Landsat	1975–2006	Band ratios VIS–NIR with thresholds and manual digitization of debris-covered glaciers
Himachal Pradesh and Uttarkand	Topographic maps	1962	Manual digitization
	IRS LISS II and IV	2001, 2002, 2004	VNIR–SWIR band combinations (2, 3, 4 and 2, 4, 5)
Himachal Pradesh	ASTER	2002	Manual digitization of glacier outlines
	SRTM	2000	DEM differencing for volume change detection
	SPOT	2004	

PAN = panchromatic; VNIR = visible near-infrared; SWIR = shortwave infrared.

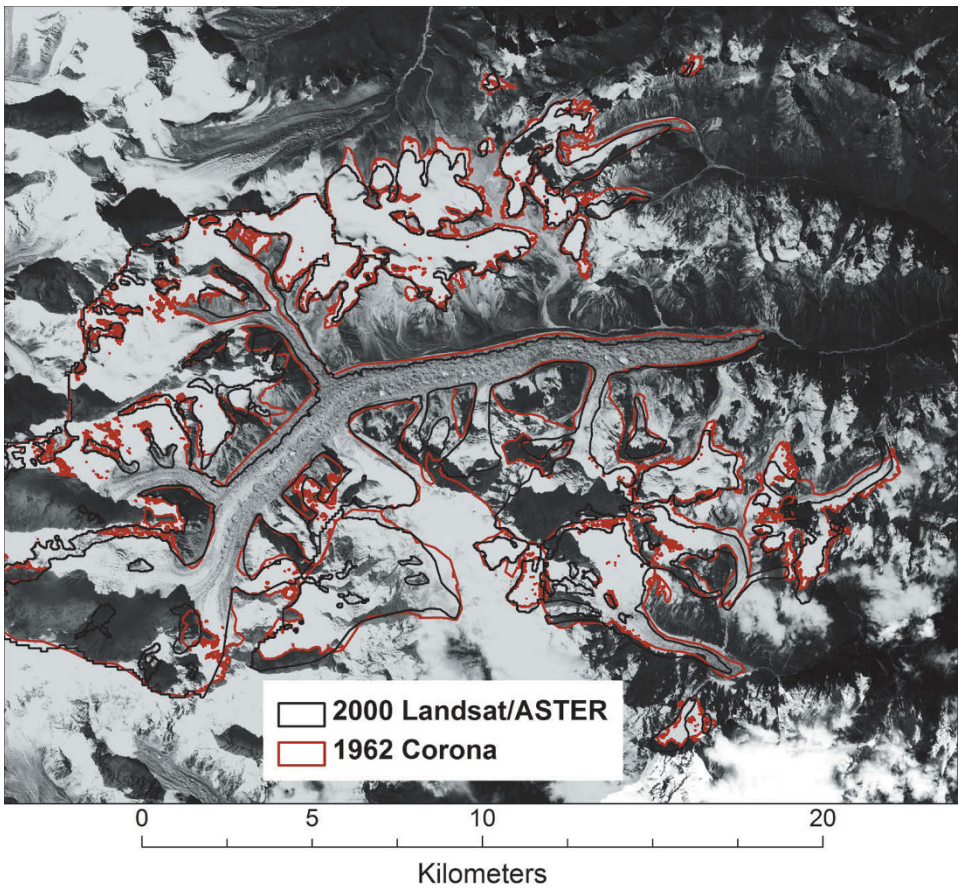

Figure 24.2. Glacier area change 1962–2000 in the Zemu area of the Sikkim Himalaya. The two sets of outlines are shown on a color composite using ASTER bands 4, 3, 2. Figure can also be viewed as Online Supplement 24.1.

receive maximum rainfall in the summer. In Nepal, about 70–80% of the precipitation occurs during the summer months. Annual precipitation recorded near Khumbu Glacier, at ~5,000 m, varies between 400 and 500 mm (Tartari et al. 1998). In addition, the Garhwal area receives precipitation in the winter from western disturbances, with maximum snowfall occurring from December to March (Dobhal et al. 2008). Among the larger glaciers in these study areas are Gangotri Glacier (area ~142 km^2), Satopanth Glacier (~21 km^2), and Bhagirathi Kharak Glacier (~31 km^2) in Garhwal, and the Khumbu (length ~17 km), Nuptse (~6 km), Lhotse (~7 km), and the Lhotse Shar/Imja Glaciers (~6km) in the Solo Khumbu study area. The ablation zones of the larger valley glaciers such as Gangotri and Khumbu are covered by thick debris. The termini of debris-covered glaciers extend about 300–400 m lower in elevation than the termini of clean glaciers. Maximum elevations in these areas reach 8,848 m at the summit of Everest in Khumbu, and 7,756 m at the summit of Kamet in Garhwal. The precise location of the termini of active debris-covered glaciers is not clearly identifiable. Velocity measurements, however, indicate that these tongues may contain some stagnant ice at the front (Bolch et al. 2008b, Quincey et al. 2009).

24.3.2.2 Methods

Glacier area change was investigated from multi-temporal remote-sensing data of various types and spatial/spectral resolutions, spanning more than four decades. Details on these sensors are provided in Table 24.1. All satellite images were ortho-rectified using the ASTER DEM generated from 2001–2003 scenes (averaged to reduce uncertainties), in conjunction with ground control points (GCPs) collected in the field. Clean glaciers were mapped from multispectral ASTER imagery using standardized techniques (e.g., application of NIR/SWIR band ratios and a threshold applied to the resulting image). We used two ASTER scenes from 2001 and 2006 for Khumbu and Garhwal, respec-

tively, to extract glacier outlines using band ratio techniques. Shadows hampered the correct identification of some glaciers in the Garhwal Himalaya. Similarly, debris-covered glacier tongues were not detected by the band ratio algorithm, so these areas were mapped manually and validated on the basis of high-resolution datasets acquired from the same years (IKONOS, Cartosat-1, and IRS LISS). The baseline dataset was constructed from panchromatic 1968 Corona images by manual on-screen digitization.

Glacier volume change for the Everest area was estimated using multitemporal digital elevation models constructed from stereo Corona KH4 and KH4B imagery (from 1962 and 1972, respectively), and stereo ASTER and Cartosat-1 (2007) imagery (Bolch et al. 2008b, 2011). For the ASTER DEM, we averaged ASTER elevations from 2001, 2002, and 2003, based on "relative" DEMs. We used relative ASTER DEMs rather than "absolute" elevations due to known errors in the latter. The estimated accuracy of relative ASTER DEMs, calculated as vertical root mean square errors ($RMSE_Z$), with respect to field GCPs was 9.6 m (Bolch et al. 2008b). We focused on calculating volume change in the debris-covered Khumbu, Nuptse, Lhotse Nup, and Lhotse Glaciers in the last four decades.

24.3.2.3 Results

The glacierized area of Garhwal Himalaya decreased from 600 ± 10.2 km^2 in 1968 to 572.5 ± 15.4 km^2 in 2006, which represents an area loss of 4.6% or ~0.12% yr^{-1} in 38 years (total percentage loss divided by number of years). Analysis of a sample of 29 selected glaciers for the 1968–1990 period revealed a loss of 3.5 ± 0.1 km^2 (3.5% or 0.16% yr^{-1}) in glacier area. Area loss for the same subset of glaciers was 5.7 ± 0.1 km^2 (5.9% or 0.37% yr^{-1}) for the 1990–2006 period, which is about double the rate of the 1968–1990 period (Bhambri et al. 2011). The number of glaciers increased from 1968 (82 glaciers) to 2006 (88 glaciers) due to glacier disintegration. Smaller glaciers (<1 km^2) lost 19.4% (~0.51% yr^{-1}) of their ice area over the whole time period (1968–2006), which contrasts with glaciers >50 km^2 losing only 2.8% of their area in the same time period (~0.07% yr^{-1}). There was no significant influence of median and mean glacier elevation, glacier aspect, or slope on the rate of glacier shrinkage in the study area.

We found a significant increase in the debris-covered area of glaciers in Garhwal from 1968 to 2006 (+14% area growth, +0.37% yr^{-1}). Based on high-resolution Corona and Cartosat-I images, we found that Gangotri Glacier lost only 0.38 km^2 (0.01 km^2 yr^{-1}) from 1968 to 2006 at its terminus. These results are in agreement with ground measurements reported by the Geological Survey of India. Srivastava (2004) reported that the terminus of Gangotri Glacier lost only 0.58 km^2 (~0.01 km^2 yr^{-1}) between 1935 and 1996. Kargel et al. (2011), drawing on their new ASTER image analysis and earlier published data for Gangotri Glacier, reported highly variable retreat rates during the 19th through the 21st centuries. They gave an average rate from 1960 to 2010 of about 7,500 m^2 yr^{-1} (0.0075 km^2 yr^{-1}). They also showed a decreasing terminus retreat and area loss rate for the 1960–2010 period, consistent with what Raina (2009) reported, but this decreasing rate was attributed to multidecadal fluctuations of Gangotri Glacier rather than a long or climatically significant secular slowdown of retreat. The more climatically significant point is that Gangotri Glacier has been retreating since the Little Ice Age, and this retreat apparently reflects both the natural warming after the LIA and more recent anthropogenically driven climate change. Similarly, Bhagirathi Kharak Glacier in the Alaknanda Basin lost an area of 0.13 km^2 (0.4%) during a similar time period (Nainwal et al. 2008). In contrast, the clean ice-covered area at the terminus of Satopanth Glacier decreased by 0.31 km^2 (1.5%) between 1962 and 2006.

In the Everest region, the ice-covered area decreased by $5.3 \pm 2\%$ (~0.12% yr^{-1}) between 1962 and 2005. Similar to Garhwal, the rates of area loss were smaller (~0.09% yr^{-1}) for the 1962–1992 period and higher (~0.25% yr^{-1}) from 1992 to 2001. Area loss was driven by shrinkage of the clean ice area (0.24% yr^{-1}), while the debris-covered area increased by +0.06% yr^{-1} (Table 24.2) (Bolch et al. 2008b). Similarly, Salerno et al. (2008) reported a slight overall decrease in glacier area (4.9% or 0.12% yr^{-1} from the 1950s to the 1990s) on the basis of historic topographic maps. The snouts of debris-covered glaciers of the Everest region such as those of Khumbu, Lhotse, or Nuptse Glaciers were found to be stable during our investigation period. Previous studies in the Everest area have shown that debris-free glaciers in the Nepal Himalaya have receded since the middle of the 19th century, but parts of debris-covered glaciers remained as stagnant ice (Iwata 1976). Other studies based on analysis of 1960 and 1975 data

Table 24.2. Change in total ice cover, clean ice, and debris-covered ice areas in the Khumbu Himalaya between 1962 and 2005 based on spaceborne imagery (source: Bolch et al. 2008b).

Year (sensor)	*Ice extent* (km^2)			*Period*	*Change rate* (km^2 yr^{-1})			*Change rate* (% yr^{-1})		
	Total area	*Clean ice*	*Debris cover*		*Total area*	*Clean ice*	*Debris cover*	*Total area*	*Clean ice*	*Debris cover*
1962 (Corona)	92.26	56.54	35.73	1962–2005	−0.11	−0.13	+0.02	−0.12	−0.24	+0.06
1992 (Landsat TM)	89.69	54.63	35.05	1962–1992	−0.09	−0.064	−0.02	−0.09	−0.11	−0.06
2001 (ASTER)	87.64	51.59	36.05	1992–2001	−0.23	−0.34	+0.11	−0.25	−0.62	+0.32
2005 (ASTER)	87.39	50.8	36.60	2001–2005	−0.11	−0.13	+0.02	−0.12	−0.24	+0.06

inventories also showed that most glaciers retreated during that time period (Higuchi et al. 1980), with likely accelerated retreat during the 1980s (Yamada et al. 1992).

Surface thinning of glaciers in the Everest area ranged from 11 m (Lhotse Glacier) to nearly 17 m on average (Khumbu Glacier) from 1962 to 2002 (Fig. 24.3). All glaciers in this area showed similar behavior (Bolch et al. 2008b, 2011): stagnating termini and slight downwasting. Downwasting was more pronounced in the middle part of glaciers, where it averaged >20 m (0.5 m yr^{-1}) but there were maxima exceeding 50 m (1.25 m yr^{-1}), and less pronounced in the upper debris-covered active part of the glacier. These results are in agreement with studies by Kadota et al. (2000) and Nuimura et al. (2012). These trends of stable termini are in contrast with the behavior of debris-covered glaciers in the Garhwal Himalaya, which experienced both downwasting and snout recession from 1960 to 2000.

24.3.2.4 Summary of findings

Glaciers in both the Garhwal and Khumbu Himalaya show area loss of ~0.12% yr^{-1} in the last 40 years based on the analysis of Corona and ASTER images. The rate of change probably accelerated in the last 20 years or so in both areas (representing a ~50% higher change in area than occurred between the 1960s and 1990s). In both study areas, clean glaciers displayed the greatest area loss, while debris-covered tongues were more stable. Average surface thinning of glaciers in the Everest area (Khumbu, Nepal Himalaya) ranged from 11 to 17 m, with stagnant termini and slight downwasting, contrary to trends found in the Garhwal Himalaya (downwasting simultaneous with snout retreat). The area loss of glaciers, coupled with glacier surface thinning in the central and eastern Himalaya may lead to the formation of new proglacial lakes in this area. This poses potential dangers for glacier lake outburst floods (GLOFs) (Bolch et al. 2008a), highlighting the need for ongoing monitoring of glacier behavior in this area.

24.3.3 Everest region, Nepal: geomorphologic and surface reflectance changes, 2001–2005

24.3.3.1 Introduction

The previous section presented glacier volume changes in the Khumbu region of the Nepal Himalaya by subtracting a DEM produced using 2001–2003 ASTER scenes from a Corona DEM based on 1962 stereo imagery. The resulting elevation difference map of some areas of Khumbu Glacier showed a surface thinning of about 40 cm yr^{-1}, on average (Bolch et al. 2011). DEM subtraction has become the standard technique for estimating changes in glacier surface using satellite images, provided that the co-registration of images and correction of elevation biases is carefully done (Nuth and Kääb 2011, Gardelle et al 2012b). Glacier surface changes based on DEM differencing were documented in several studies in the Himalaya (Berthier et al. 2007, Bolch et al. 2008b) and elsewhere (Racoviteanu et al. 2008). Other surface change detection techniques are based on using multispectral image correlation, radar interferometry, and speckle-tracking to derive surface displacement vectors on glaciers over a given interval of time, as demonstrated by Bolch et al. (2008b) and Quincey et al. (2009) for the Khumbu area. Glacier

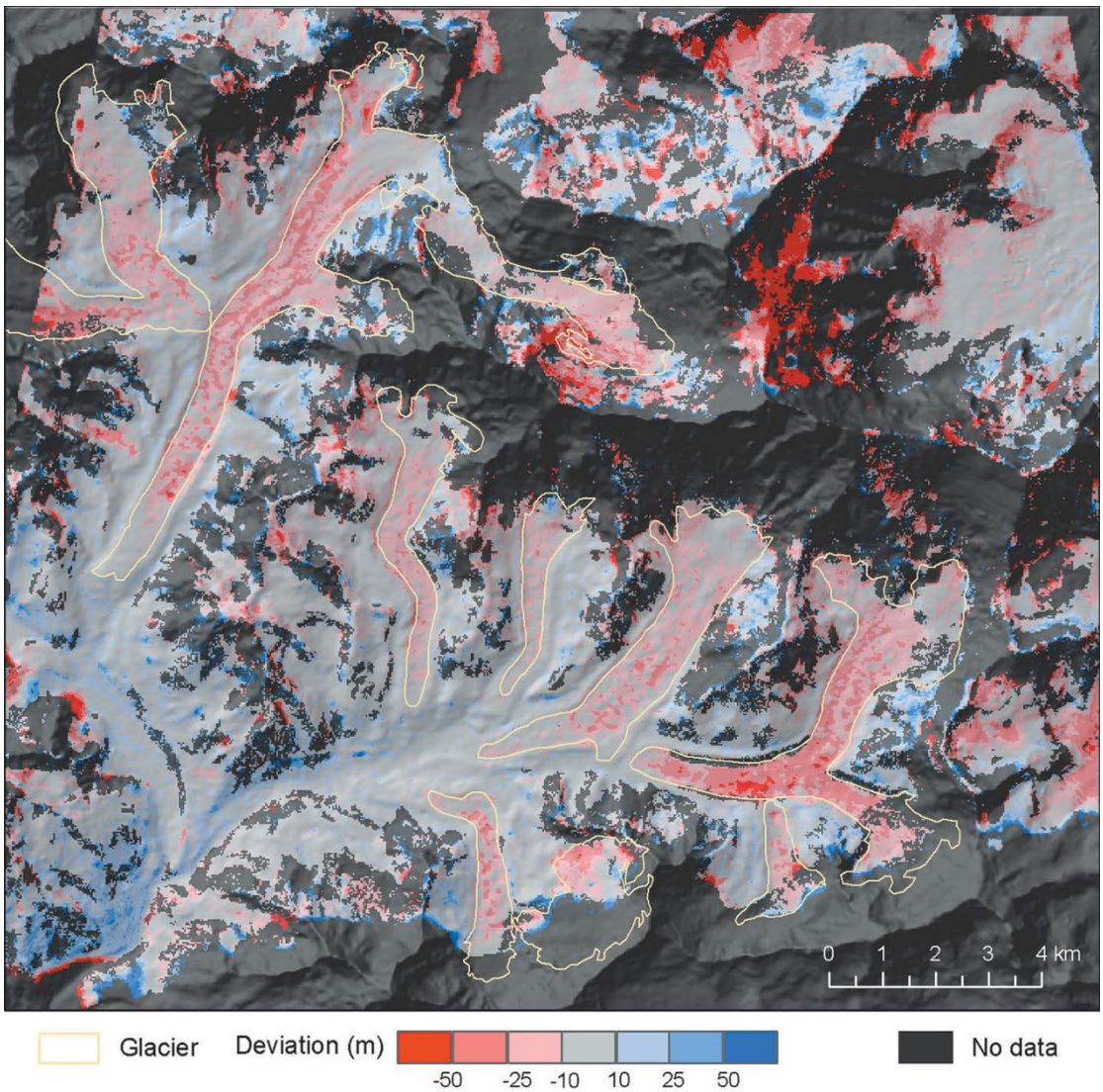

Figure 24.3. Glacier elevation changes 1970–2007 at Mt. Everest calculated from a Corona KH-4B DEM and a Cartosat-1 DEM (source: Bolch et al. 2011). Figure can also be viewed as Online Supplement 24.2.

velocity changes have been estimated from satellite imagery in a few areas of the Himalaya (Kääb 2005, Quincey et al. 2009). Accurate results from multitemporal imagery, however, require some preprocessing steps such as topographic and atmospheric correction, which is difficult to perform and has the disadvantage of introducing errors in change estimates. Changes in glacier surfaces are relatively easy to detect in areas where lateral movement of terrain due to glacial flow, collapse, changes in ground cover, or any other topographic changes have occurred. These areas appear uncorrelated on any two differenced multitemporal images, even if they are acquired under similar illumination conditions. However, if the illumination geometry or phase angle of two observations differ substantially, apparent differences in radiance are not transformed accurately to differences in reflectivity, because the photometric properties of surfaces caused by various object sizes may dominate radiance differences. In such cases, there is generally not enough information to apply a transformation with sufficient accuracy so that image differencing can work.

24.3.3.2 Methods

Here we have taken a simpler and more reliable

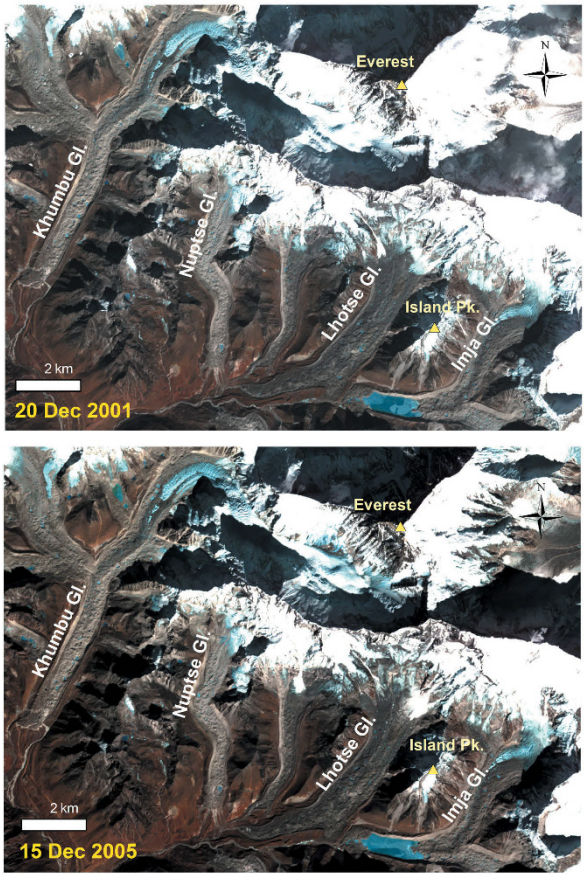

Figure 24.4. A subset of ASTER 321RGB false-color composite images of the Mt. Everest area showing earlier 2001 (top) and later 2005 (bottom) images. The 2001 image was subtracted from the 2005 image to produce a differenced image: Fig. 24.5. Figure can also be viewed in higher resolution as Online Supplement 24.3.

approach to solving this problem, one which however requires observations to be made when the Sun is in the same position in the sky, using the same phase angle. This implies using scenes obtained on similar dates, and from the same nadir view in different years, which is not always feasible. For this study, excellent repeat ASTER imagery around the Mt. Everest area in Nepal allowed selecting two very high-quality images (near 0% cloud and haze coverage, and low snow coverage), acquired almost exactly four years apart (December 20, 2001 and December 15, 2005). Most importantly, the images were acquired only five (calendar) days apart, and <4 minutes in time of the day, ensuring almost identical illumination conditions. Additionally, the instrument gain settings and view angles of this image pair were also the same, so that the images appear almost identical except in glacierized areas, glacier lakes, and snowfields. The change that occurred in these areas is readily discerned in the scaled radiance space of the differenced images, without first having to perform any transformation to reflectance (Fig. 24.4). We evaluated glacier change by subtracting the 2001 scaled radiance image from the 2005 image (Fig. 24.5). Further technical details of this methodology (ICESMAP), constraints, and limitations are provided in Section 4.7.2 of this book by Kääb et al. In this chapter's Appendix (Section 24.5) we provide details on the analysis of this specific image pair and the errors associated with its ICESMAP processing.

24.3.3.3 Results

We interpret change at the glacier surface as:

(1) *Glacier flow discerned from the effects of change in aspect and slope*: the pattern of hill shading and illumination on glacier surfaces shifts as a result of ice flow that has occurred between image capture dates. In areas where the local surface of the glacier was either uniformly covered by debris or was uniform bright ice or snow but undulating and flowing, the subtraction image shows most of these features as a mottled grayscale component that dominates many glaciers. The various mottled shades of gray occur not because the spectrum has shifted, but the pattern and intensities of photometric shading and illumination associated with small undulations has been displaced as a function of multitemporal shifts in aspect and slope at or greater than the pixel scale.

(2) *Change in position of supraglacier ponds and ice*: areas where small supraglacial ponds once existed are marked by red on the difference image. The red areas are caused by subtracting pixels showing where the pond was in 2001 (blue) from the 2005 image, thus producing red areas. Blue has been added to the pond's new location, causing a blue area to appear on the difference image. Ponds and patches of blue ice that are moving hence appear as paired red and blue areas, with the blue zones juxtaposed downglacier from the red. Assuming no change in pond size, the distance and direction between the centroids of the red and blue spots indicates the local surface displacement vector. Note that our analysis does not produce vectors or flow velocities, but simply highlights areas where

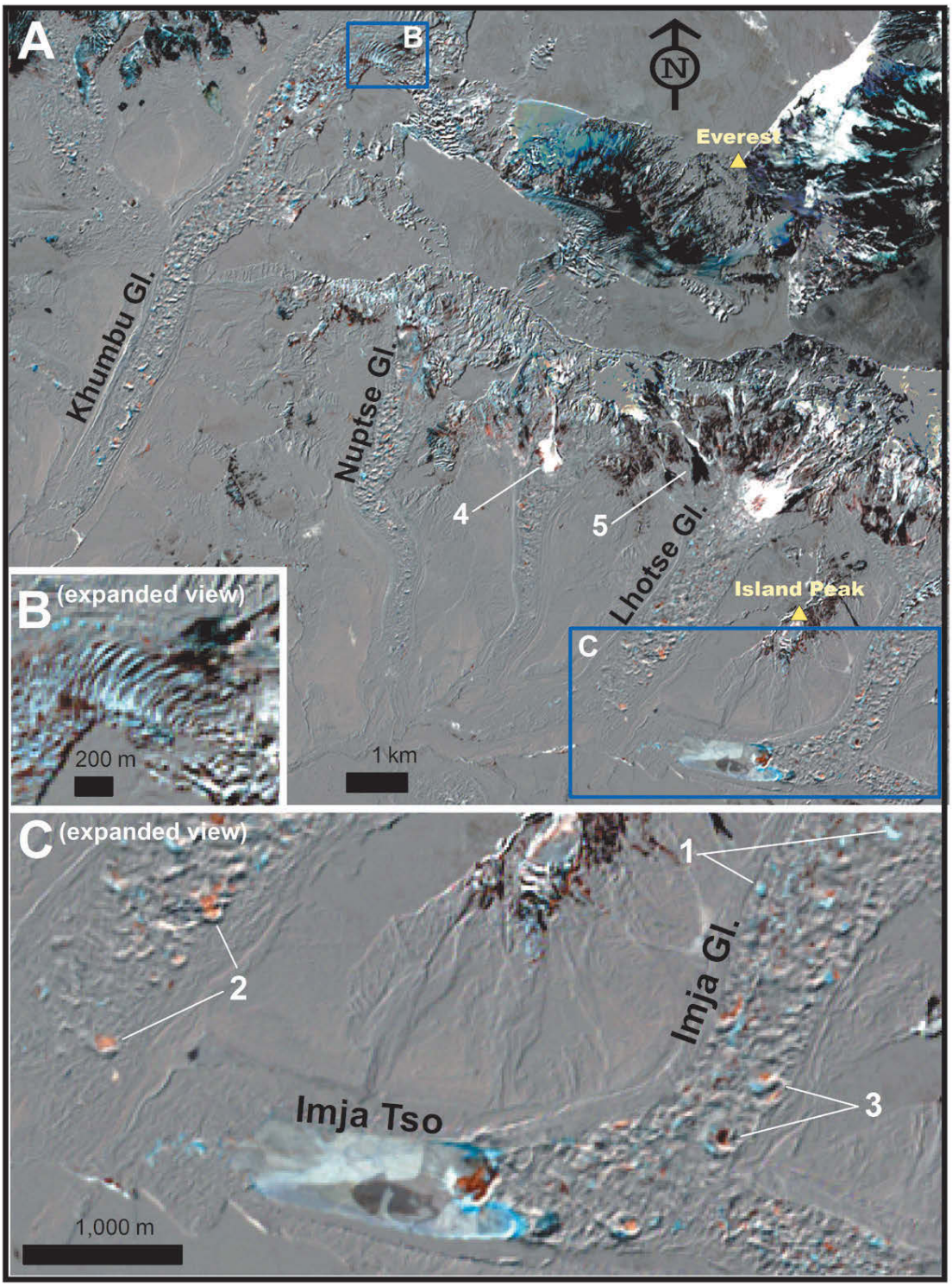

Figure 24.5. (A) and (C) Sagarmatha–Khumbu region, Nepal. ASTER 321RGB false-color composite: December 2005 minus December 2001. Note the annotated features where (1) new supraglacial ponds have appeared (single blue zone); (2) ponds have disappeared (single red zone); (3) supraglacial ponds or blue ice patches have shifted, producing a paired blue–red zone; (4) new snow avalanches appear in couloirs as white zones; (5) reexposed rock in couloirs appears black. (B) Ogives appear as rhythmic bands of alternating contrast. Figure can also be viewed in higher resolution as Online Supplement 24.4

glaciers or lakes are very active, less active, or stagnant. In summary, the disappearance of ponds is marked by red areas on the subtraction image, and new ponds are represented by blue patches.

(3) *Ogives and crevasse swarms*: these features are given away by their surface oscillations and feature a combination of components such as relief, ice microstructure, and variable debris-to-ice ratio. They tend to appear in the subtraction image as banded patterns alternating blue and red or banded patterns with different tones of grayscale.

(4) *Snow, ice, and rock exposures*: areas covered with snow in 2001, which were exposed as blue ice in 2005, appear as dark-gray or dark-blue patches. Black pixels generally represent areas that changed from snow to rock. On the other hand, 2001 rock areas, which later received snow from avalanches, appear as white areas on the subtraction image. Large snow avalanches may have occurred in the intervening years between the two images. Snowline retreat from 2001 to 2005 is visible as black areas on many glaciers.

(5) *Glacier and moraine-dammed lakes*: lakes that were variably covered by ice each year or experienced changes in water turbidity appear as red, blue, green, white, and black mosaics.

24.3.3.4 Summary of findings

In summary, the pixel colors on the subtraction image (Fig. 24.5 and Online Supplement 24.4) are indicative of the type of spectral change that occurred over a period of 4 years, which in turn is key to specific surface changes. The overall texture of gray and colored mottlings (speckle) indicates areas where glaciers and other surfaces have been most active. In areas where glaciers appear as untextured neutral gray colors, there has been little spectral change. Glaciers in this case appear to be stagnant, or otherwise may have experienced only subpixel (<15 m) displacement over the intervening years between image acquisitions. Note that undetected surface changes may occur in some cases, including changes within areas that are beyond sensor spatial resolution. This may happen, for example, within zones of very clean smooth ice that undergoes basal sliding. However, if such a zone is bounded by ice and/or debris of higher contrast, which shows displacement on the difference image, movement within the contained clean ice zone may be inferred. Most long-valley glaciers, such as Khumbu, were fairly stagnant near their termini, had broad lateral inactive zones, and central cores of more active ice. Conversely, Imja Glacier appears to be active right up to its calving and retreating margin along Imja Lake, as detected by the patches of red and blue indicating glacier lake growth and positional shifting.

The multispectral image change detection techniques presented here have the potential to provide an initial indication of the type of material involved in surface change (e.g., snow, ice, debris, and water). Optimal use of this type of information can complement the other types of change assessment presented above, including flow speed and topographic changes. As discussed in Section 24.5 (Appendix), applying these methods routinely would require an observation program designed to acquire images of glaciers in a study area on a yearly basis, on or near anniversary dates. Such a program is currently not in place with the present spaceborne sensors, given the complicated logistics and difficulties of acquiring high-quality images in some areas of the Himalaya due to clouds and snow. Hence, GLIMS should be tasked with creating a next-generation observing system.

24.3.4 Brahmaputra River basin: glacier area, volume, and velocity changes, 1970s through to about 2000

24.3.4.1 Introduction

In this section we summarize the results of the BRAHMATWINN project. Our objective is to enhance and improve the capacity to carry out an integrated water resource management plan for the Brahmaputra River basin. Our study areas include northwest Brahmaputra, Nepal (hereafter referred to as "NW"), the Nyainqentanglha Range, Tibet/China ("Lhasa"), and the Wang Chu Basin, Bhutan ("Wang Chu") (Fig. 24.1).

24.3.4.2 Methods

As part of this project, current glacier distribution and glacier change since the 1970s were investigated using multitemporal optical remote-sensing data from Landsat, ASTER, and Corona. Repeat glacier outlines were combined with the SRTM DEM and analyzed within a GIS to assess change in glacier area. New glacier outlines were derived from Landsat ETM+ data from 2000. The Chinese Glacier

Inventory (CGI) served as the baseline dataset for change detection based on 2000 glacier data. The CGI was constructed using 1974 aerial photos (NW) and 1970 aerial photos (Lhasa). Glaciers in the NW and Lhasa areas were mapped semiautomatically using the band ratio approach presented in detail by Paul et al. (2002) and Racoviteanu et al. (2009). Initially, Landsat TM4/TM5 band ratios were computed, from which binary glacier masks were created by interactive thresholding. On the dry northern slopes of the Himalaya, the threshold value for the ratio image was ~2.5. A 3×3 median filter was applied to the binary image to reduce noise, and the resulting raster areas were finally converted into vector data. These vector data consisted of large contiguous ice masses, which were divided into individual glaciers by intersecting the data with a vector layer of glacier basins. The glacier basin layer was digitized manually using the Landsat ETM+ as a baseline to discern glacier basins and ice divides. Wherever possible, the CGI data were also used as for reference purposes. Visual inspection of glaciers and associated glacier basins was used as an additional information source. The resulting vectors of individual glaciers were compared with CGI glacier outlines to find misalignments (due to georeferencing) or digitizing errors in the CGI. Misclassification typically occurs for wetlands, lakes, and rivers erroneously classified as ice, as well as for the lack of classification for medial and lateral moraines. Errors due to cast shadow (induced by the steep relief) and debris cover on glaciers were corrected manually. Glacier outlines for the Wang Chu Basin were obtained by manual digitization of 1974 Corona data and 2000 Landsat data. Manual digitization was preferred over semiautomatic approaches in this basin due to the small number of glaciers and widespread debris cover, which hampers the use of band ratio techniques.

24.3.4.3 Results: glacier area change

The procedures described above resulted in the identification of 197 glaciers for the NW area and 476 glaciers for Lhasa, which we used for change analysis. Table 24.3 and Fig. 24.6 show glacier area and volume change for two of the study areas, NW and Lhasa, respectively. Our study yielded glacier area loss rates of 0.9% yr^{-1} in northwest Brahmaputra (1974–2000), 0.7% yr^{-1} in the Lhasa River area (1970–2000), and 0.6% yr^{-1} in Wang Chu Basin (1974–2000) (compounded interest formula). Differences in the rates of retreat among the regions can partly be attributed to the varied distribution of glacier size in the study areas, as well as different climatic conditions (monsoon influences), the degree of debris cover, and different glacier hypsometries. Our results are in good agreement with area changes reported from other studies. For example, in the Pumqu Basin (Tibet), Jin et al. (2005) found mean glacier area losses of 0.8% yr^{-1} for the period 1970–2001, while Karma et al. (2003) found mean glacier area reductions of the order of 0.9% yr^{-1} for the period 1963–1993 for Bhutan. Note the significant discrepancy between our results and another recent study in the Lhasa River area (Bolch et al. 2010). Our estimate of area losses (19.8% over the period 1980–2000) is clearly larger than that reported in Bolch et al. (2010) (6.1 ± 3.1% total area loss for 1976–2001). We believe the main reasons for this difference lie in uncertainties associated with the baseline inventory (CGI) and in the different methods used to correct inaccuracies in each study.

Table 24.3. Glacier area/volume change in the northwest Brahmaputra Basin (Area 1) and the Lhasa River basin (Area 2). Reference glacier outlines are from the Chinese Glacier Inventory (Area 1: aerial photos from the 1970s, Area 2: the 1980s). Glacier outlines from 2000 are based on Landsat data. Volume estimates are based on two empirical relations between glacier area and mean glacier depth.

Area	*Glacier area* (km^2)		*Area change 1970/1980–2000*		*Glacier volume* (km^3)		*Volume change 1970/1980–2000*	
	1970/1980	*2000*	*km^2*	*%*	*1970/1980*	*2000*	*km^3*	*%*
Area 1	449.4	372.6	−76.7	−17.1	12.9[a]/27.7[b]	10.6/22.4	−2.3/−5.3	−17.6/−19.3
Area 2	535.3	429.5	−105.8	−19.8	13.0/19.6	10.4/15.6	−2.6/−4	−20.0/−20.3

[a]Maisch (1992).
[b]Driedger and Kennard (1986).

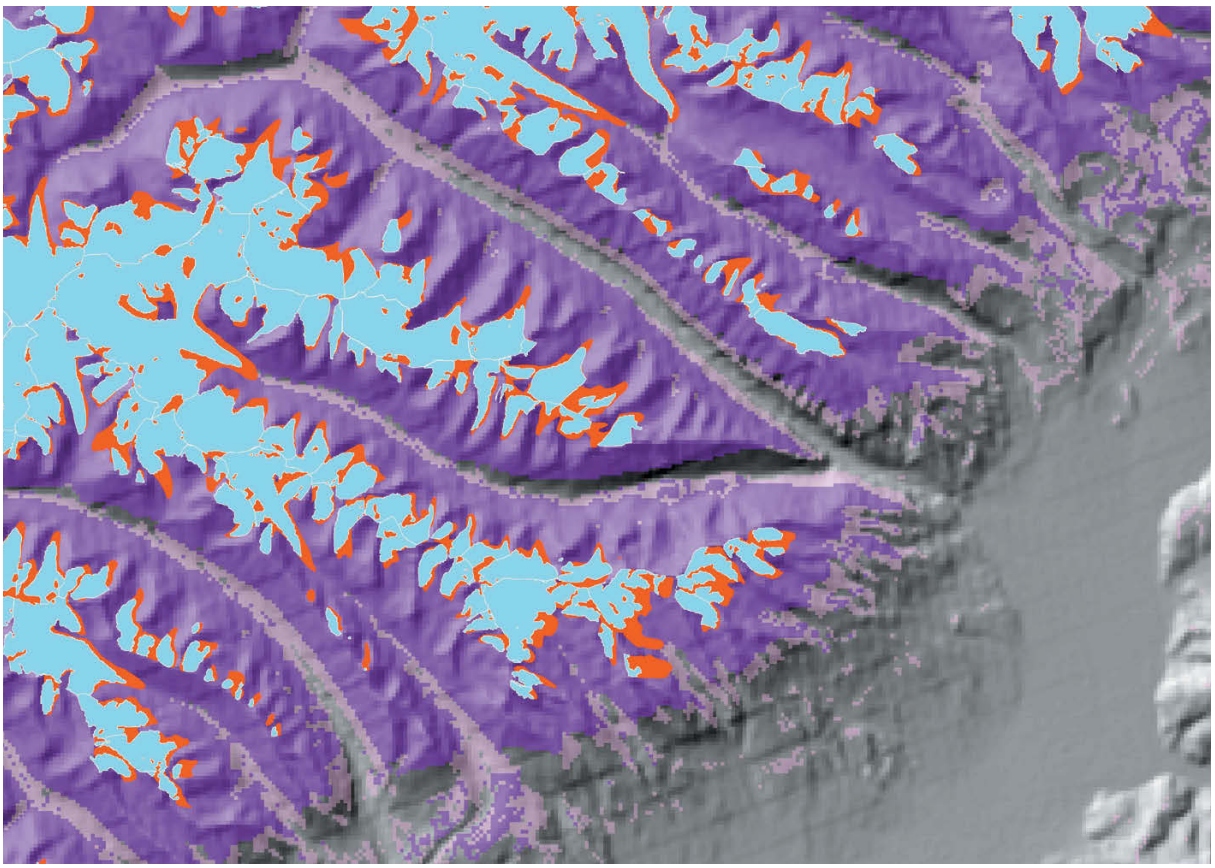

Figure 24.6. Glacier change in the Lhasa River basin between 1970 and 2000. (Blue) Glaciers as mapped from Landsat data of 2000. (Red) Glacier areas lost since 1970 (CGI). (Light and dark violet) Probable likely permafrost distribution as modeled following an approach by Keller (1992), adjusted using regional meteorological data. The hillshade in the background is based on the SRTM DEM. Stripes in the hillshade stem from nearest neighbor interpolation during reprojection. Figure can also be viewed as Online Supplement 24.5.

24.3.4.4 Results: glacier volume change

Since glacier volume cannot be measured directly using spaceborne multispectral imaging, we used two different empirical relations between glacier area and mean glacier thickness to estimate glacier volumes: one developed by Maisch (1992) and the other by Driedger and Kennard (1986). Both relations are based on radar measurements of glacier thickness and the areas of the glaciers investigated. The results of these two methods are presented in Table 24.3 for the NW and Lhasa areas, and show large discrepancies in volume estimates between the two methods. However, these approaches for glacier volume estimation can provide rough first-order estimates. We estimated an upper-range volume loss of ~20% between the 1970s and 2000, or an average of roughly 0.3–0.4 m water equivalent loss per year (Lhasa area) (Table 24.3). Although absolute volumes according to the two approaches differ greatly, the difference in volume change estimates is about the same. When volume change is comparably small, the errors in both approaches are comparable for both points in time and any error in volume difference is eliminated. Assuming that glacier change in these three study regions is representative of the entire Brahmaputra Basin, we upscaled our area change results using the CGI and size class–specific area changes. These assumptions gave area loss of the order of 13% per decade since the 1970s, or volume loss of 7 km^3 w.e. per year (0.02 mm yr^{-1} sea level equivalent) for glaciers in the Brahmaputra catchment. Our findings suggest that glaciers in the three study regions of the Upper Brahmaputra River basin have lost roughly 20% of their water-equivalent ice reserves during the last 20–30 years.

24.3.4.5 *Results: glacier velocities*

The surface velocity field of glaciers is an important variable for glacier inventorying, monitoring, and hazard assessment. We investigated ice flow velocities in Lunana (~28°N, 90–91°E), the northernmost section of the Bhutan Himalayan main ridge, separating the Tibet Plateau to the north from the central Himalaya to the south (Fig. 24.1). The lowest terrain is 3,700 m, located south of the main ridge. The northern sections approaching the Tibetan plateau have minimum elevations of around 5,000 m, with the highest peaks around 7,300 m. Most glaciers north of the divide are oriented to the north, and most glaciers south of the divide to the south. The glacier tongues we investigated are found at minimum elevations of 5,000 m to the north, and 4,000 m to the south of the main Bhutan watershed.

We derived horizontal displacements of individual glacier features from multitemporal ASTER orthoimages using CIAS (the Correlation Image Analysis Software; Kääb and Vollmer 2000). Double cross-correlation based on the gray values of images was used to identify corresponding areas on both images. Figs. 24.7 and 24.8 show surface speeds between January 2001–October 2002 and January 2001–November 2001, respectively (Kääb et al. 2005). Glacier tongues on the northern and southern slope differ in topographic and surface characteristics as well as dynamics. Northbound glaciers originate from large ice plateaus up to 7,000 m asl, while southbound glaciers originate from steep ice and rock faces having relatively small accumulation areas. These steep headwalls provide a sustained supply of rock debris that covers the southern glaciers, whereas such debris accumulation is not significant for northern glaciers. In addition to being debris covered, southbound glacier tongues contain thermokarst features such as rapidly changing depressions and supraglacial ponds. In their terminus zones, glacier speed is near

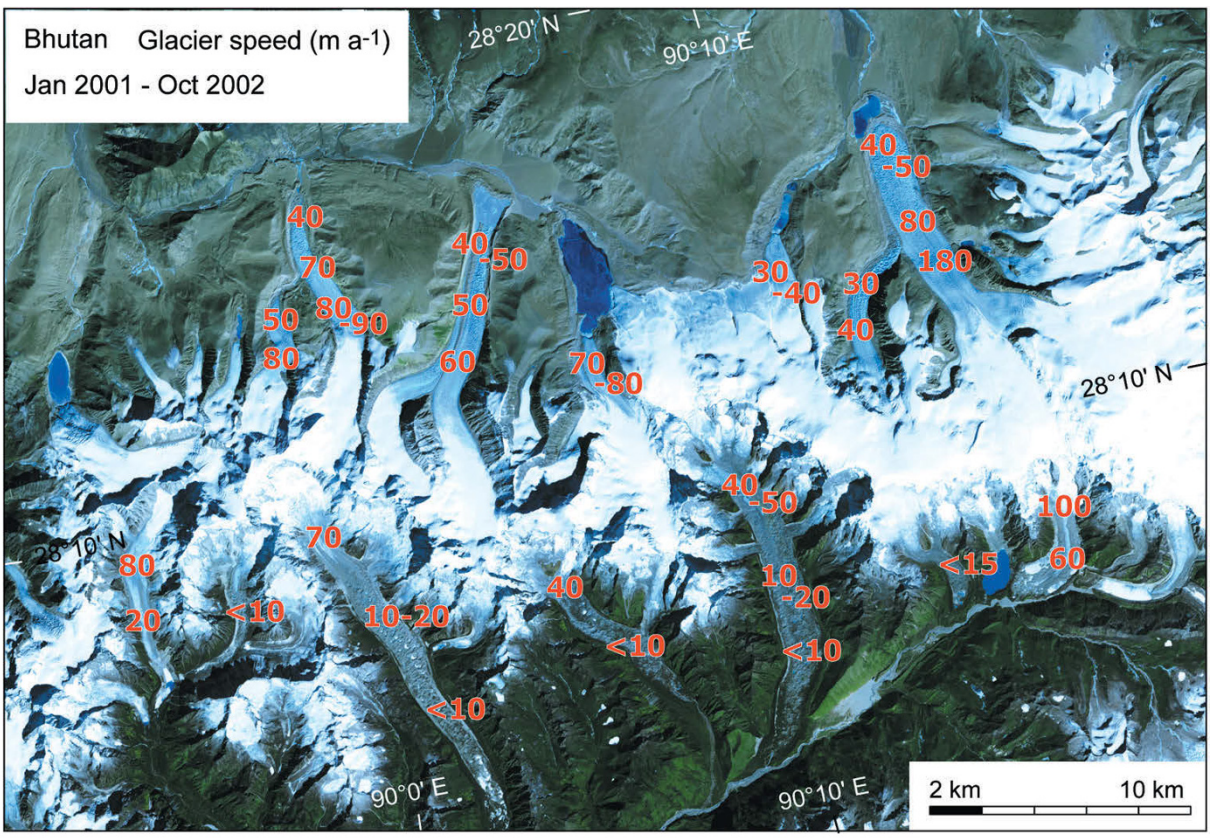

Figure 24.7. Velocities are derived from repeat ASTER data of 2001 and 2002. Northbound glaciers flow significantly faster than debris-covered southbound glaciers. For a detailed look at the upper-right glacier (for a subset period) see Fig. 24.8 (background image: ASTER 321 RGB composite with R converted to green to simulate natural colors).

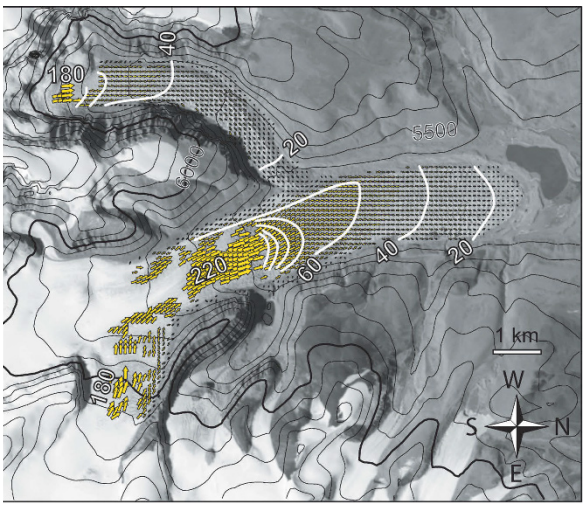

Figure 24.8. Velocity field (vectors) and isolines of speed of a glacier in Bhutan (upper-right glacier in Fig. 24.7) as derived from repeat ASTER data of January 20, 2001 and November 20, 2001 (background image is an ASTER 3N orthoimage with SRTM elevation contour lines overlaid).

the noise level of the image-matching techniques applied (i.e., in the range of 10–20 m yr^{-1}). Higher speeds are only reached at steep glacier gradients above the tongues.

Northbound glacier tongues showed speeds ranging from several tens to over 200 m yr^{-1} (Fig. 24.8). These high speeds combined with steep transverse gradients at the margins imply large amounts of basal sliding. Well-preserved crevasses over the observation period also indicate minimal stress variations. Northern glaciers have almost no debris cover. Their light-blue ice color in ASTER VNIR RGB false-color composites indicates a relatively high content of air bubbles refracting the sunlight. Fast-flowing glacier tongues could well reflect balance velocity (i.e., the ice flux needed to drain the relatively large glacier accumulation areas through the northbound valleys in order to keep glaciers in a state of equilibrium). The surface slopes of southern and northern glacier tongues were of the order of a few degrees. Surface speed for similar slopes was clearly higher for northern glaciers. Thus, different surface slopes can largely be excluded as the reason for the large speed differences observed. Speed differences point to different basal processes and higher balance velocities. The uniform and relatively high speed found at glacier tongues in the throes of calving might also be linked to lake water pressure reducing basal drag. The low speeds found at southern glacier tongues indicate that the delivery of ice to large sections of the tongues is in short supply. Such reduced ice flux supports the development of pronounced differential melt, such as results from supraglacial ponds and other thermokarst features. Low speeds enhance the accumulation of debris on the glacier surface through reduced debris transport and proglacial deposition.

24.3.4.6 Summary of findings

Our analysis of Landsat ETM data from 2000 and old CGI inventory data point to glacier area losses of 0.9% yr^{-1} in northwest Brahmaputra (1974–2000), 0.7% yr^{-1} in the Lhasa River area (1970–2000), and 0.6% yr^{-1} in Wang Chu Basin (1974–2000). Glacier volume reduction was estimated as 13% over the last three decades, on the basis of area–thickness scaling and upscaling of the three basins in the Upper Brahmaputra River basin analyzed here. Glacier velocity analysis in the Lunana region of Bhutan showed speeds ranging from several tens to over 200 m yr^{-1} for northern slopes, while southern tongues appear to be nearly stagnant. Today's (2013) expected response to atmospheric warming for these glacier tongues is downwasting, which is essentially decoupled from the dynamics of the upper-glacier zone. Under certain topographic circumstances, some southern glacier tongues could potentially lose contact with upper-glacier zones and become detached dead ice. As a consequence, enhanced development of glacial lakes on and at southern glacier tongues coupled with an increase of related hazards may be expected under conditions of continued atmospheric warming. In contrast to southern glaciers, northern glacier tongues are fast flowing. Most likely, these glaciers will dynamically adjust to climate variations and thus respond to atmospheric warming by retreating rather than by local decaying. The process of glacier retreat is enhanced by calving processes in areas where glacier tongues terminate in lakes. The high ice velocities of glacier tongues in the Lunana area are an efficient and thus important component of ice mass turnover within these glaciers. Therefore, variation in the long-term mass balance of northern glaciers will likely be reflected by changes in ice speed.

24.3.5 Ladakh, northwestern Indian Himalaya: glacier length/area change, 1975–2008

24.3.5.1 Introduction

Ladakh, including the two districts of Leh and Kargil, makes up more than half of the Indian State of Jammu and Kashmir in the northwestern part of India (Fig. 24.1). The rugged topography has an average elevation of over 3,000 m, with its highest points at Nun (7,135 m) and Kun (7,077 m) in the Greater Himalaya range. The town of Leh is the capital of Ladakh (now the Leh District). At an elevation of 3,506 m it receives mean annual precipitation of only 93 mm (Archer and Fowler 2004). Hence, as also observed in the field, the local population is dependent on snow and glacier meltwater for irrigation and consumption. The Greater Himalaya range in the south of Ladakh blocks most Indian summer monsoon precipitation. As a result, aridity generally increases toward the north, and valley glaciers are more numerous and larger in the southern Greater Himalaya and Zanskar ranges. In the northern Ladakh range, cirque glaciers are more common than valley glaciers (Zgorzelski 2006). The equilibrium line altitude for glaciers is situated between 5,200 and 5,400 m. These glaciers are mostly oriented in a northwest to northeast direction (Burbank and Fort 1985).

24.3.5.2 Methods

Let us take a look at the work of Byrne (2009) and Kamp et al. (2011), who analyzed glacier length and area change between 1975 to 2006 in Ladakh. The two studies included, among others, the smaller Himis-Shukpachan Glacier (area: 0.96 km^2; length: ~2 km) in the Ladakh range and 13 long-valley glaciers in the Greater Himalaya range between the Nun Kun and Zanskar Massifs; also among them is the ~23 km long Drang Drung Glacier and the ~12 km long Parkachik Glacier. Geomorphological field mapping and GPS observations of glacier termini were conducted in the summers of 2007 and 2008. ASTER DEMs were generated using SilcAst 1.07 software, without GCPs. Cuartero et al. (2005) estimated the accuracy of SilcAst-generated ASTER DEMs without GCPs as ~6 m at that time, reported as $RMSE_Z$ with respect to 40 individual checkpoints (CPs). Toutin (2008) considered this accuracy to be good enough in most DEM analyses. Snow and ice-covered areas were mapped using a geomorphometric mapping approach making use of Landsat and ASTER imagery, including NIR/SWIR band ratios, thermal information, supervised classification, cluster analysis of surface morphology, and visual image interpretation. Manual editing was necessary to delineate the debris-covered parts of glaciers, since semiautomated methods are often not accurate enough for multitemporal mapping (Kamp et al. 2011). The relative percentage of debris cover on glacier tongues was taken into account when quantifying glacier changes.

24.3.5.3 Results

In the Ladakh range, the smaller Himis-Shukpachan Glacier receded by ~75 m (−9 m yr^{-1}) between 2000 and 2007 (Table 24.4). In the Greater Himalaya range there was also a general glacier retreat between 1975 and 2008, although

Table 24.4. Change in length and debris-covered area for three glaciers in Ladakh.

Glacier name	*Length 2007/2008* (km)	*Period*	*Change in length* (m)	*Change in length* (%)	*Change in debris-covered area* (%)
No name (Himis-Shukpachan, Ladakh Range)	2	2000–2007	−75	−3.8	
Drang Drung (Greater Himalaya)	23	1975–2008 1990–2004	−311	−1.3	 +10
Parkachik (Nun Kun Massif; Greater Himalaya)	13	1979–1990 1990–2004 2004–2008	−141 +179 −7	−1.1	 +8

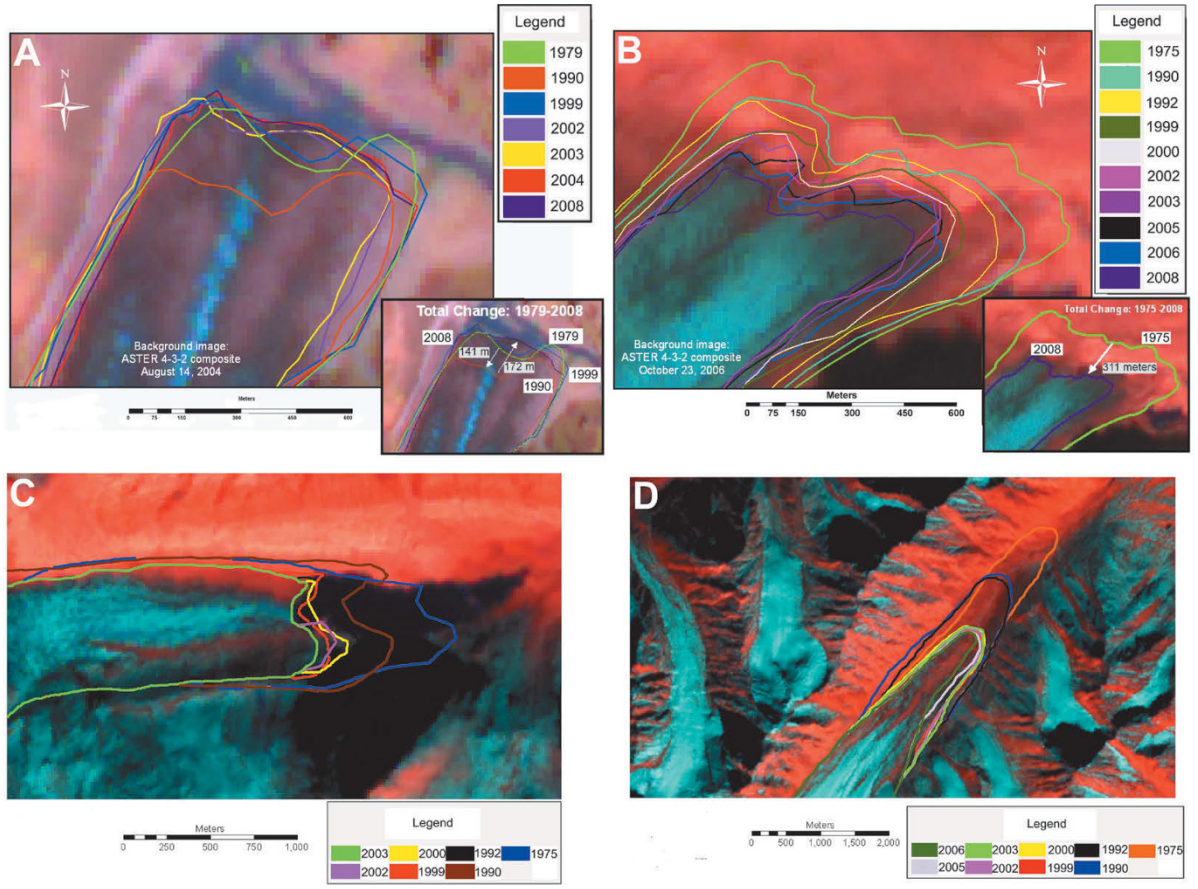

Figure 24.9. Glacier change results based on semiautomated mapping approaches: (a) Parkachik Glacier (SA-3); (b) Drang Drung Glacier (SA-4); (c) Glacier 4 (SA-5); (d) Glacier 10 (SA-5). Figure can also be viewed in higher resolution as Online Supplement 24.6. Source: Kamp et al. (2011).

differences in the fluctuations of individual glaciers exist. Glacier margin change rates were +4 to −60 m between 1975 and 1992, −2 to −89 m between 1992 and 2002, and +11 to −52 m between 2002 and 2006. Besides this general trend towards negative glacier budgets, there were times when "glacier-feeding" conditions occurred locally between 1975 and 2008: 1 of the 13 glaciers advanced significantly, 9 showed at least minor advances, and only 3 failed to advance at all. For example, Drang Drung Glacier receded ~311 m (−9 m yr^{-1}) (Fig. 24.9), but its debris-covered area increased by >10% between 1990 and 2006. In contrast, Parkachik Glacier exhibited fluctuating patterns: a retreat of ~141 m (−13 m yr^{-1}) between 1979 and 1990, an advance of ~179 m (+13 m yr^{-1}) between 1990 and 2004 (Fig. 24.9), and a further retreat of 7 m (−2 m yr^{-1}) between 2004 and 2008. Despite the 1990–2004 advance, Parkachik Glacier's debris-covered area increased by ~8% (+0.6% yr^{-1}). This is in stark contrast to other areas, where decrease in the debris-covered area of ablation zones was noted for glaciers that experienced mass gain (Stokes et al. 2007, Bolch et al. 2008b).

24.3.5.4 Summary of findings

The two studies summarized here concluded that glaciers in Ladakh have generally been receding since the 1970s, although fluctuations between individual budget years are common. One exception to this trend was Parkachik Glacier, which, after a period of retreat in the 1980s, experienced rapid advance in the 1990s and early 2000s. This anomalous behavior might be due to its specific topographic character: (i) it is steep, has an impressive icefall, and extends down from Nun Kun Massif into the Suru River which continuously erodes the glacier terminus, thereby obliterating differences in glacier margin positions; and (ii) Nun Kun

Massif might be trapping much of the precipitation from westerlies during the winter, preferentially feeding Parkachik Glacier on the northern slope. Hewitt (2005) also reported a number of glaciers in the Pakistani Karakoram as anomalously advancing due to topographic factors. While some of these trends may be a result of climate change, some fluctuation may specifically be due to local topographic circumstances, rather than climatic changes. Further work is required to understand the contributions from both effects to glacier size.

24.3.6 Himachal Pradesh and Uttarakhand, western Indian Himalaya: glacier area change, 1962–2004

24.3.6.1 Introduction and methods

The earliest information about glacial extent in the Indian Himalaya is available from Survey of India topographic maps at 1:50,000 scale, which were constructed from aerial photos and field investigations dating from 1962. In this study, we used maps from 1962 to construct a baseline glacier dataset, which was then compared with new glacier outlines from 2001/2002/2004 LISS-II/LISS-IV images for area change detection. We selected images from July to September, when snow cover was minimal and glacier ice was mostly exposed. Snow and ice had high spectral reflectance values in VIS bands 2 and 3 of IRS LISS-II and LISS-IV sensors, and lower reflectance values than vegetation in NIR band 4, allowing glacier and nonglacier areas to be differentiated. Remote sensing-based glacier outlines were derived using standard VIS–NIR band combinations (bands 2, 3, 4) from LISS-II and IV images, respectively, combined with visual interpretation techniques. Debris-covered parts of glaciers were difficult to identify using multispectral analysis alone, and required geomorphologic features such as moraine-dammed lakes that tend to form downstream of glacier termini (Fig. 24.10) to be used as auxiliary data to indicate glacier termini. The extents of glaciers terminating in lakes are more easily identified on satellite images. Depending on illumination geometry, icewalls at the glacier terminus cast shadows in the downstream direction, which can be used as markers for terminus delineation (Bahuguna et al. 2007). Field investigations were carried out at Shaune Garang Glacier (Baspa Basin), Parbati Glacier (Parbati Basin), and Chhota Shigri, Samudra Tapu, and Patsio Glaciers (Chenab Basin) to validate snout position using a GPS. The relative position of the terminus was compared with geomorphologic features such as

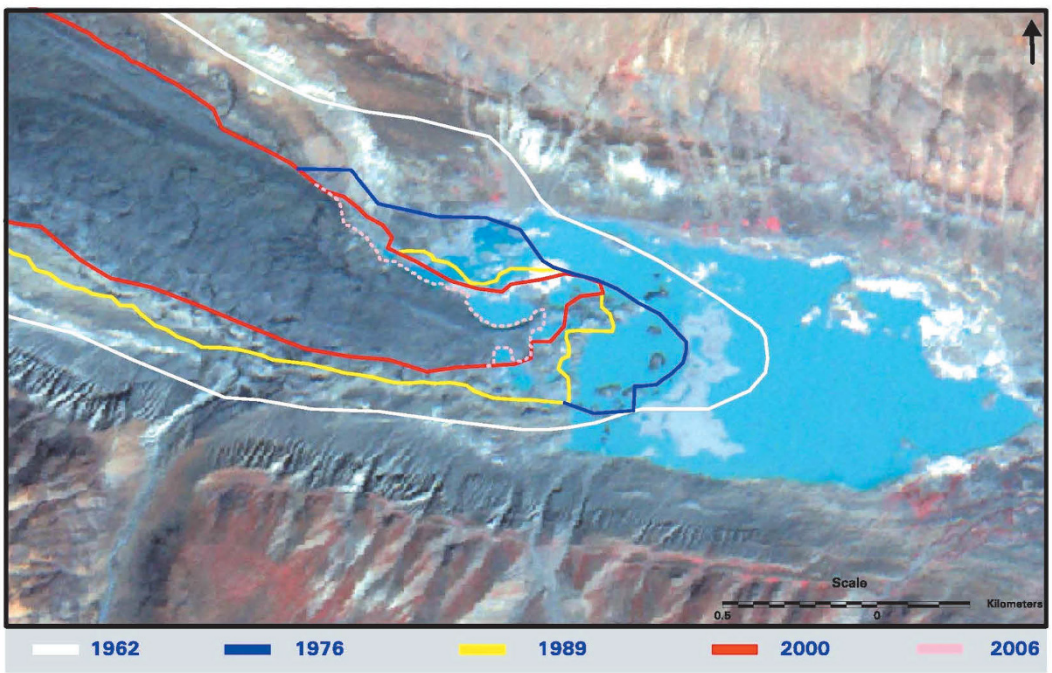

Figure 24.10. Retreat of Samudra Tapu Glacier, Himachal Pradesh between 1962 and 2006. IRS LISS IV imagery: September 16, 2006.

Table 24.5. Glacier retreat in Himachal Pradesh and Garhwal Himalaya from 1962–2001/2004.

Basin	*No. of glaciers*	*Area 1962* (km^2)	*Area 2001/2004* (km^2)	*Area change 1962–2001/2004* (%)
Chandra	116	696	554	−20
Bhaga	111	363	254	−30
Parbati	90	493	390	−20
Basapa	19	173	140	−19
Warwan	253	847	672	−21
Bhut	189	469	420	−10
Miyar	166	568	523	−8
Alaknanda	126	734	638	−13
Bhagirathi	187	1,218	1,074	−11
Gauriganga	60	305	256	−16
Total	*1,317*	*5,866*	*4,921*	*−16*

moraines, origin of stream from the glacier snout, and moraine-dammed lakes. Changes in glacier length were measured along the centerline of the glaciers visible on satellite images, using GIS tools.

24.3.6.2 Results

The results showed there were 1,317 glaciers covering a total area of 5,866 km^2 in 1962. The area decreased to 4,921 km^2 in 2001/2004, an overall area loss of 16% for this time period. Glacier area loss values are given in Table 24.5. An example of glacier change is shown in Fig. 24.10 for the debris-covered tongue of Samudra Tapu Glacier. The degree of glacier retreat varies from glacier to glacier and from basin to basin, depending on parameters like maximum thickness, mass balance, and rate of melting at the terminus (Kulkarni et al. 2005). In addition, the loss of glacierized area depends on glacier size (Kulkarni et al. 2007), possibly because glacier response time is directly proportional to thickness (Johannesson et al. 1989), and thickness is directly proportional to areal extent (Liu and Sharma 1988). Glacier response time is known as the amount of time a glacier requires to adjust to a change in its mass balance. For small glaciers (<1 km^2) in the Himalaya that are not heavily covered by debris, the rate of surface melting at the snout is around 6 m yr^{-1} and the response time is estimated as between 4 and 11 years (Kulkarni et al. 2005). Other factors being equal, small glaciers are expected to react faster to climate change. This has been observed in our study area, where glaciers smaller than 1 km^2 lost almost 38% of their area between 1962 and 2001/2004. By contrast, larger glaciers (>10 km^2) lost only 12% of their area during the same period. At the same time, the numbers of glaciers increased as a result of disintegration (Fig. 24.11).

24.3.6.3 Summary of findings

In this chapter we have estimated glacier area loss in the Parbati River basin, Himachal Pradesh (Indian Himalaya) from the 1960s to the 2000s on the basis of topographic maps and LISS-II/LISS-IV imagery. We have estimated area loss of 16% over the 40-year period (0.4% yr^{-1}) in this area of the western Himalaya, with rates per individual basin ranging from 0.2 to 0.7% yr^{-1}. Wide variability in the degree of area loss from basin to basin depends on parameters such as maximum glacier thickness, mass balance, and rate of melting at glacier termini (Kulkarni et al. 2005). Note, however, that the rate

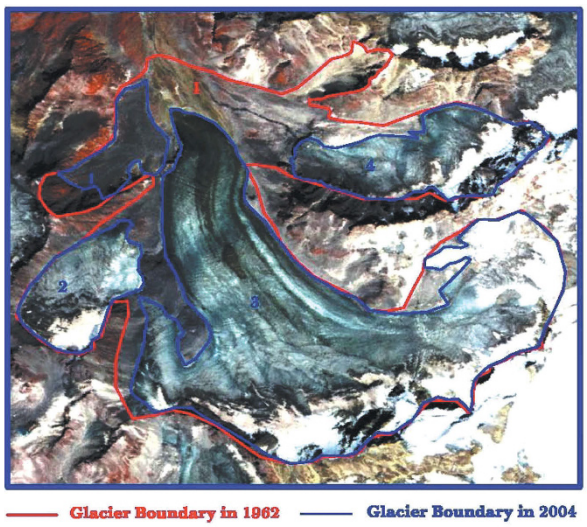

Figure 24.11. Disintegration of glaciers in the Parbati River basin, Indian Himalaya.

of area loss in Himachal Pradesh is overall smaller than loss rates noted in Sikkim, eastern Himalaya in this chapter (0.7% yr^{-1} for the same time period) (Section 24.3.1), or ~0.5% yr^{-1} for the central Himalaya (Garwhal and Nepal) (Section 24.3.2). We have also estimated that smaller glaciers (<1 km^2) lost almost 38% of their area between 1962 and 2001/2004 (~0.9% yr^{-1}). This is in contrast with larger glaciers (>10 km^2), which have lost only 12% (~0.3% yr^{-1}) during the same period. At the same time, as noted in other areas of the Himalaya, the numbers of glaciers increased as a result of disintegration. Future steps include improving termini position assessment by means of laser range finder and GPS measurements, which will help provide more accurate positions of glacier termini and much-needed validation of methodologies based on remote sensing.

24.3.7 Himachal Pradesh, western Himalaya: geodetic mass balance estimates, 1999–2004

24.3.7.1 Introduction

The mass balance of Himalayan glaciers is poorly sampled in the field, and there are but few estimates based on remote sensing. In an effort to fill this void gap, we conducted the first space-based measurement of glacier elevation change by monitoring glacier mass balances in the Lahaul-Spiti region of the Indian Himalaya (Figs. 24.1 and 24.12). The annual mass balance of Chhota Shigri Glacier (16.5 km^2) has been measured in the field since 2002 using a network of stakes and pits located between 4,300 and 5,500 m elevation. Surveys were carried out each year at the end of the ablation season (late September/early October) (Wagnon et al. 2007).

24.3.7.2 Methods

Elevation change was obtained by comparing a DEM derived from 2004 SPOT imagery with the 2000 SRTM DEM following a procedure developed and validated in the French Alps (Berthier et al. 2004). The 2004 DEM was derived from two SPOT-5 satellite optical images without any ground control points (due to the accurate onboard geolocation of SPOT-5 scenes). SRTM elevations were used as a reference for ice-free zones. Glacier outlines were manually digitized from a cloud-free ASTER image acquired on September 28, 2002 and absorbed into the GLIMS database. Before comparing glacier surface elevations, the two DEMs were co-registered and evaluated on non-glacierized areas surrounding the glaciers, where no elevation change would be expected. We found that long-wavelength bias affected the SPOT-5 DEM and was correlated to an anomaly in the roll (i.e., rotation about an imaginary axis from nose to tail) of the SPOT-5 satellite. An additional bias was observed as a function of altitude and was attributed to the SRTM dataset. Both biases were modeled and removed by precise adjustment of the SRTM DEM and the SPOT-5 DEM to allow unbiased comparison of the two DEMs on the 915 km^2 ice-covered area.

24.3.7.3 Results

A thinning of 4 to 7 m was observed in the lower and middle parts of glaciers in Himachal between 4,400 and 5,000 m in elevation, which included debris-covered tongues (Fig. 24.13). Elevation change was smaller in the upper reaches of the glaciers (only slight thinning of about 2 m). Elevation change was converted to volume change using the hypsometry of each glacier. The conversion of volume change to mass balance requires knowledge of the density of the material lost or gained. This is straightforward in the ablation zone where ice (density 900 kg/m^3) is involved, but more problematic in the snow-covered accumulation zone, where density varies between that of snow and ice (about 100 to 900 kg/m^3). To resolve this, we computed mass balance using two density values of the material lost in the accumulation zone (ice or snow). We assumed an ELA of 5,100 m, as determined in the

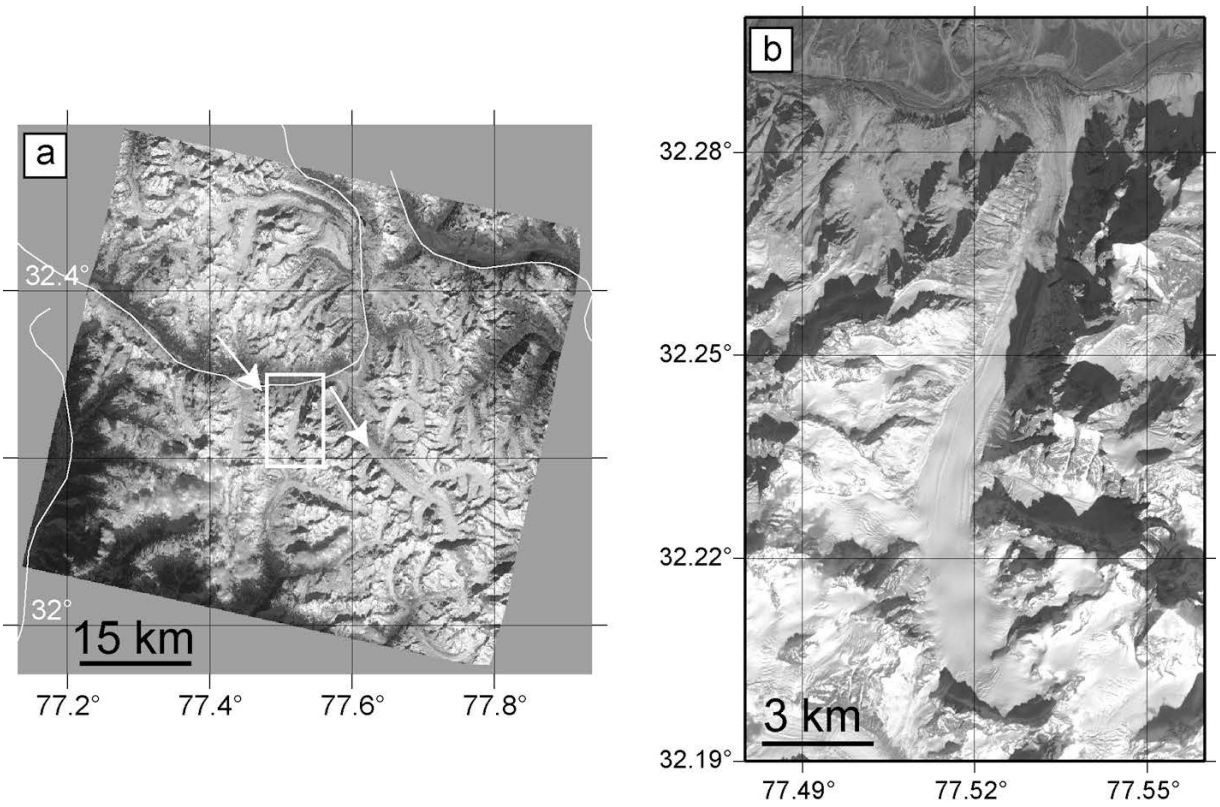

Figure 24.12. (a) November 12, 2004 SPOT-5 image of the Chhota Shigri area, Lahaul-Spiti, showing the main rivers. The arrows indicate Chhota Shigri and Bara Shigri Glaciers and the white rectangle locates the Chhota Shigri Glacier shown in greater detail in (b). Note the shadows cast by steep valley walls and the low solar illumination in late autumn.

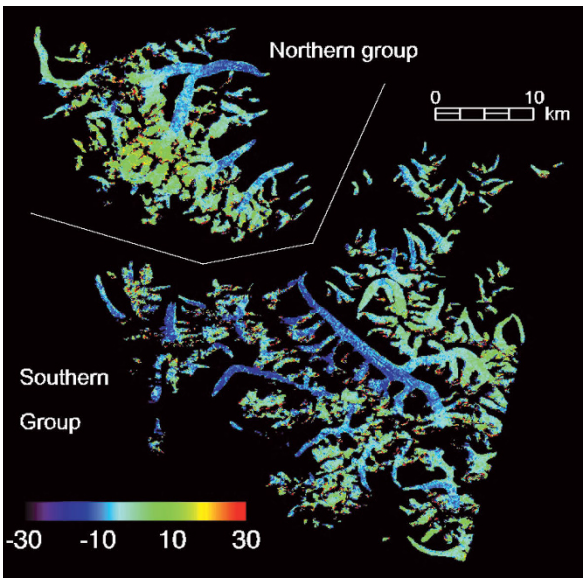

Figure 24.13. Map of glacier elevation change (in meters) between February 2000 and November 2004 for glaciers in the Lahaul/Spiti region.

field for Chhota Shigri Glacier during hydrological years 2002–2003 and 2003–2004. We obtained an average annual mass balance of 0.7 to 0.85 m yr^{-1} w.e. for the period 1999–2004, depending on the density values used for material lost (or gained) in the accumulation zone. The uncertainty associated with elevation change and mass balance is difficult to quantify given the lack of simultaneous ground measurements. Furthermore, the penetration of the SRTM C-band radar in snow and ice, which can reach up to 10 m, induces elevation-dependent biases which require corrections of the glacier elevations (Gardelle et al. 2012b). However, there is reasonable agreement between remote-sensing estimates (1 to 1.1 m yr^{-1} w.e. from 1999 to 2004) and field estimates (1.13 m yr^{-1} w.e. from 2002 to 2004) for the mass balance of Chhota Shigri Glacier.

24.3.7.4 Summary of findings

In this chapter we have demonstrated the use of spaceborne DEM data to derive relatively accurate

estimates of glacial mass balance in a remote area of northern India (Berthier et al. 2007). These measurements are crucial to monitoring in a more effective way the flux of mass balance of Himalayan glaciers in response to climate change, and to estimate its contribution to water resources. This remote-sensing methodology will be of increasing value in the near future with the availability of new satellite DEMs. Future DEM data, with increasingly greater time separation from SRTM DEMs, will provide for a clearer signal-to-noise ratio and insure that average mass balance estimates will be more robust.

24.4 SUMMARY AND OUTLOOK

This chapter presented the current understanding of Himalayan glacier change in the last few decades, using remote sensing and topographic maps. The contributions in this chapter specifically focused on change in glacier area and thickness, in velocity and mass balance, and the amount of water glaciers donate to streamflow. Most contributions relied on semiautomatic methods for glacier delineation, but encountered topographic shadowing effects as well as difficulties with water bodies and debris cover, which had to be corrected manually. Applying standard image processing and terrain analysis techniques poses challenges in the Himalaya due to the complex terrain and lack of field measurements for validation.

The technical conclusions drawn with respect to remote-sensing algorithms include

- combining multitemporal remote-sensing data of various types and spatial resolution (ASTER, Landsat TM, Corona, Cartosat, and LISS) proved useful in the compilation of new glacier inventories for the Himalaya, where a single sensor might be limited by cloud cover or gain settings as well as by spectral or spatial resolution;
- band ratios (NDSI and single-band) were the most common methods used by the coauthors to delineate glaciers over large areas of the Himalaya, with some manual adjustment for clouds, water bodies, and debris-covered glaciers;
- political restrictions imposed on early Indian topographic maps of border regions posed a challenge in deriving estimates of glacier change based on remote-sensing imagery—some coauthors successfully used Corona imagery as a baseline dataset for comparison with new imagery, after correcting distortions in the Corona scenes;
- the void-filled SRTM DEM was used by most coauthors to estimate glacier thickness change, and infer the mass balance of Himalayan glaciers at the decadal scale;
- uncertainties in glacier change estimates were inevitable considering the lack of information about the accuracy of early topographic maps used in the study.

The conclusions drawn from contributions in this chapter with respect to spatiotemporal glacier change in the Himalaya in recent decades include

- glacier area change (loss) ranged from 0.1% yr^{-1} in Ladakh (western Himalaya) and Garhwal (central Himalaya) to ~0.4% yr^{-1} in Himachal Pradesh (western Himalaya) and ~0.5% yr^{-1} in Sikkim (eastern Himalaya) in the last three decades;
- annual rates of glacier area change in the dry areas of the western Himalaya (Ladakh) are generally up to seven times higher than the wet monsoon-dominated eastern Himalaya (Sikkim);
- glacier area change accelerated in the 1990s compared with the previous three decades in Garhwal (three times as great) and Ladakh (twice as great);
- smaller glaciers (<1 km^2) lost more percent area than larger glaciers for the same time period, whereas long-valley glaciers covered with thick debris appeared to be generally stagnant;
- increase in the debris-covered area of glaciers was noted in the Garhwal, Khumbu, and Ladakh Himalaya concomitantly with clean glacier ice loss;
- glacier volume loss was estimated to be of the order of 20% in the last three decades in Brahmaputra Basin, central Himalaya.

Future work on the Himalaya needs to focus on removing the uncertainties involved in glacier change estimates, extending glacier volume and mass balance estimations to larger scales, and understanding the effect of larger circulation patterns on glacier mass balance.

24.5 APPENDIX—IMAGE DIFFERENCING: METHODOLOGY, LIMITATIONS, AND ERRORS

A more detailed description of the methodology for this type of application is presented in Chapter

4. The ASTER images used include identically subset portions of AST14DMO_00312202001050229 and AST14DMO_00312152005045832 scenes, collected on December 20, 2001 and December 15, 2005, respectively (see Section 24.3.3; Fig. 24.4). Preprocessing for these on-demand products includes radiometric calibration and geometric co-registration of image bands; output includes at-sensor radiance given in $W/m^2\ \mu m^{-1}\ sr^{-1}$ and then rescaled into 8-bit DN values (King et al. 2003). Subsequent to this, VNIR bands 3, 2, and 1 were stacked into an image cube and rendered into RGB color space at full ASTER VNIR spatial resolution (15 m) for each image. The image pair was co-registered using several ground control points selected from the images. Subpixel accuracy for relative co-registration between the image pair was achieved ($RMSE_{x,y} = 4.4$ m). The DN values of the later image were subtracted from the DN values of the earlier, and the residual 8-bit image was rescaled in DN, yielding an image with a minimum DN of 0 and maximum DN of 255. The rescaled DN = 0 represents terrain that had undergone maximum change from bright in 2001 to dark in 2005; the rescaled DN = 255 represents maximum shift from dark in 2001 to bright in 2005. Unchanged terrain, whether it is snow, rock, water, or ice, appears as neutral gray on the subtraction image due to this DN rescaling. The results of image differencing (Fig. 24.5) include mostly real surface changes, but there are also the following artifacts:

(1) *Shadow shift*: the 5-day difference in time of year means that the vector to the Sun is not exactly the same, such that shadows have moved slightly, with some areas emerging into sunlight and others moving into shadow. As a first-order assessment of change in shadow position, we calculate that the solar zenith angle increases over a 5-day period from December 15 to December 20 by 0.36°, and the solar azimuth shifts by 0.56° (with image time of day approximated at 10:30 AM local time); for shadows of local topographic relief of 3,000 m, the shadow of a mountain peak would increase in length from 5,229 m to 5,276 m (+47 m), and the azimuthal position of the shadow peak shifts 51 m, for a total shift in location of 69 m (root of the sum of squares of two orthogonal components in shadow shift), or roughly 4.6 ASTER VNIR pixels. Shadow shift in this image pair becomes subpixel for local relief <650 m. Thus, high-frequency relief on the glacier, where local relief is of the order of 100 m or less, does not have significant shadow shift associated with changing illumination geometry. Changes shown on the glacier, in this example, are generally due to actual glacier change. The impact of this artifact in glacier areas is negligible and less than image registration error.

(2) *Shadow suppression*: another shadow-related artifact suppresses real change indicators. This occurs within shadow areas, where neutral gray tones (suggesting little change) predominate in the change image, even where real change may have occurred. The problem occurs within shadowed areas that cause low DN values. Subtraction of one small number from another small number (even if there have been intrinsic material change) results in a third small number, which then gets rescaled to a near-neutral gray. Hence, the method is not well suited to shadowed areas, though some change can locally be discerned in those areas.

(3) *Solar illumination angle*: a slight differential illumination angle can result from differences in imaging date or in variations in the degree of haze. This causes general background terrain containing stream valleys, small hills, and other features to show up faintly in the subtraction image because the solar incidence angle was not exactly the same. Sunward-facing slopes see very little impact, but antisunward slopes can experience substantial change in solar incidence angle, even when the solar elevation angle changes by a couple of degrees.

(4) *Image pair misregistration*: any slight misregistration will also result in slight ghosting of the original image but, as stated above, image misregistration for our image pair is only about 0.3 pixels. It is evident that most of the high-contrast and colored features in the change image are present near mountain summits, glaciers, and lakes, where real changes have occurred. Areas lacking glaciers, snow, and lakes, even in areas with rugged terrain, including sharp mountain crests and peaks, almost fade away to uniform neutral gray in the difference image. This suggests that all the artifacts described above, plus the failure to convert radiance to reflectance, and lack of explicit corrections for photometric phase angle effects, have very little influence on the difference image. Imaging time of day is potentially a factor to consider. However, imaging time of day for any Sun-synchronous orbiting space-

craft is controlled as long as latitude, longitude, and day of year are also controlled. This is not generally the case for different satellites. Even when different spacecraft fly in strict formation, such as Landsat 7 and Terra, there is a slight difference in acquisition time between leading and trailing orbits.

The biggest limitation of this approach is that it requires images acquired close to anniversary dates; if images are not taken on exact dates of the year, the next best results are achieved near the summer or winter solstice, when the Sun's position in the sky does not change much from day to day, as it does during equinoxes. In practice, a difference of a few days from the anniversary date has little impact on the results, but a wider time interval would cause photometric and shadow change effects to dominate over many surface material changes. An alternate option is to choose dates that are mirrored around the solstice; for instance, one image obtained 10 days before the solstice and another 10 days after the solstice in different years would ensure the Sun is in the same position in the sky. However, when the imaging day of the year varies so much, some surface changes may occur that are related to seasonality, such as differences in vegetation, which might not be of interest to glaciologists.

24.6 ACKNOWLEDGMENTS

ASTER data courtesy of NASA/GSFC/METI/Japan Space Systems, the U.S./Japan ASTER Science Team, and the GLIMS project.

24.7 REFERENCES

Ageta, Y., and Higuchi, K. (1984) Estimation of mass balance components of a summer-accumulation type glacier in the Nepal Himalaya. *Geografiska Annaler: Series A, Physical Geography*, **66**(3), 249–255.

Archer, D.R., and Fowler, H.J. (2004) Spatial and temporal variations in precipitation in the Upper Indus Basin, global teleconnections and hydrological implications. *Hydrology and Earth System Sciences*, **8**(1), 47–61.

Azam, M.F., Wagnon, P., Ramanathan, A., Vincent, C., Sharma, P., Arnaud, Y., Linda, A., Pottakkal, J.G., Chevallier, P., Singh, V.B. et al. (2012) From balance to imbalance: A shift in the dynamic behaviour of Chhota Shigri glacier, western Himalaya, India. *Journal of Glaciology*, **58**(208), 315–325, doi: 10.3189/2012JoG11J123.

Bahuguna, I.M., Kulkarni, A.V., Arrawatia, M.L., and Shresta, D.G. (2001) *Glacier Atlas of Tista Basin (Sikkim Himalaya)* (SAC/RESA/MWRG-GLI/SN/16/2001), Divecha Center for Climate Change, Indian Institute of Science, Bangalore, India.

Bahuguna, I.M., Kulkarni, A.V., Nayak, S., Rathore, B.P., Negi, H.S., and Mathur, P. (2007) Himalayan glacier retreat using IRS 1C PAN stereo data. *International Journal of Remote Sensing*, **28**(2), 437–442.

Bajracharya, S.R., Mool, P.K., and Shrestha, B.R. (2007) *Impact of Climate Change on Himalayan Glaciers and Glacial Lakes*, ICIMOD, Kathmandu, Nepal, 119 pp.

Bajracharya, S.R., Mool, P.K., and Shrestha, B.R. (2008) Global climate change and melting of Himalayan glaciers. In: P.S. Ranade (Ed.), *Melting Glaciers and Rising Sea Levels: Impacts and Implications*, Icfai University Press, Hyderabad, India, pp. 28–46.

Bajracharya, S.R., and Shrestha, B. (2011) *The Status of Glaciers in the Hindu Kush-Himalayan Region*, International Center for Integrated Mountain Development, Kathmandu, Nepal, 127 pp. ISBN: 978 92 9115 217 9.

Barnett, T.P., Adam, J.C., and Lettenmaier, D.P. (2005) Potential impacts of a warming climate on water availability in snow-dominated regions. *Nature*, **438**, 303–309.

Barros, A.P. and Lang, T.J. (2003) Monitoring the monsoon in the Himalayas: Observations in Central Nepal, June 2001. *Monthly Weather Review*, **131**, 1408–1427.

Barry, R.G. (2006) The status of research on glaciers and global glacier recession: A review. *Progress in Physical Geography*, **30**(3), 285–306.

Benn, D.I., and Evans, D.J.A. (1998) *Glaciers and Glaciations*, John Wiley & Sons, New York.

Benn, D.I., and Lehmkuhl, F. (2000) Mass balance and equilibrium-line altitudes of glaciers in high-mountain environments. *Quaternary International*, **65/66**, 15–29.

Benn, D.I., and Owen, L.A. (1998) The role of the Indian summer monsoon and the mid-latitude westerlies in Himalayan glaciation: Review and speculative discussion. *Journal of the Geological Society*, **155**(2), 353–363.

Berthier, E., Arnaud, Y., Baratoux, D., Vincent, C., and Rémy, F. (2004) Recent rapid thinning of the "Mer de Glace" glacier derived from satellite optical images. *Geophysical Research Letters*, **31**, L17401, doi: 10.1029/2004GL020706.

Berthier, E., Arnaud, Y., Vincent, C., and Remy, F. (2006) Biases of SRTM in high-mountain areas: Implications for the monitoring of glacier volume changes. *Geophysical Research Letters*, **33**(8), L08502, doi: 08510.01029/02006GL025862.

Berthier, E., Arnaud, Y., Kumar, R., Ahmad S., Wagnon, P., and Chevallier, P. (2007) Remote sensing estimates of glacier mass balances in the Himachal

Pradesh (Western Himalaya, India). *Remote Sensing of Environment*, **108**(3), 327–338.

Bhagat, R.M., Kalia, V., Sood, C., Mool, P.K., and Bajracharya, S.R. (2004) *Himachal Pradesh Himalaya India: Inventory of Glaciers and Glacial Lakes and the Identification of Potential Glacial Lake Outburst Floods (GLOFs) Affected by Global Warming in the Mountains of Himalayan Region* (report in CD-ROM format), International Center for Integrated Mountain Development, Kathmandu, Nepal, 254 pp.

Bhambri, R., and Bolch, T. (2009) Glacier mapping: A review with special reference to the Indian Himalayas. *Progress in Physical Geography*, **33**(5), 672–702.

Bhambri, R., Bolch, T., Chaujar, R.K., and Kulshreshtha, S.C. (2011) Glacier changes in the Garhwal Himalaya, India, from 1968 to 2006 based on remote sensing. *Journal of Glaciology*, **57**(203), 543–556.

Bhatt, B.C., and Nakamura, K. (2005) Charactieristics of Monsoon rainfall around the Himalayas revealed by TRMM precipitation radar. *Monthly Weather Review*, 149–165.

Bhutiyani, M.R., Kale, V.S., and Pawar, N.J. (2007) Long-term trends in maximum, minimum and mean annual air temperatures across the Northwestern Himalaya during the twentieth century. *Journal of Climatic Change*, **85**(1/2), 159–177.

Bhutiyani, M.R., Kale, V.S., and Pawar, N.J. (2010) Climate change and the precipitation variations in the northwestern Himalaya: 1866–2006. *International Journal of Climatology*, **30**(4): 535–548.

Bishop, M.P., Bonk, R., Kamp, U., Jr., and Shroder, J.F., Jr. (2001) Terrain analysis and data modeling for alpine glacier mapping. *Polar Geography*, **25**(3), 182–201.

Bishop, M.P., Shroder, J.F., Jr., Bonk, R., and Olsenholler, J. (2002) Geomorphic change in high mountains: A western Himalayan perspective. *Global and Planetary Change*, **32**, 311–329.

Bolch, T., Buchroithner, M.F., Peters, J., Baessler, M., and Bajracharya, S. (2008a) Identification of glacier motion and potentially dangerous glacial lakes in the Mt. Everest region/Nepal using spaceborne imagery. *Natural Hazards and Earth System Science*, **8**, 1329–1340.

Bolch, T., Buchroithner, M., Pieczonka, T., and Kunert, A. (2008b) Planimetric and volumetric glacier changes in the Khumbu Himalaya since 1962 using Corona, Landsat TM and ASTER Data. *Journal of Glaciology*, **54**(187), 592–600.

Bolch, T., Kang, Y.S., Buchroithner, M.F., Scherer, D., Maussion, F., Huintjes, E., and Schneider, C. (2010) Glacier inventory for the western Nyainqentanglha Range and the Nam Co Basin, Tibet, and glacier changes 1976–2009. *The Cryosphere*, **4**, 419–433.

Bolch, T., Pieczonka, T., and Benn, D.I. (2011) Multidecadal mass loss of glaciers in the Everest area (Nepal Himalaya) derived from stereo imagery. *The Cryosphere*, **5**, 349–358.

Bolch, T., Kulkarni, A., Kääb, A., Huggel, C., Paul, F., Cogley, J.G., Frey, H., Kargel, J.S., Fujita, K., Scheel, M. et al. (2012) The state and fate of Himalayan glaciers. *Science*, April 20, **336**(6079), 310–314, doi: 10.1126/science.1215828.

Bookhagen, B., and Burbank, D.W. (2006) Topography, relief and TRMM-derived rainfall variations along the Himalaya. *Geophysical Research Letters*, **33**(L08405), doi: 10.1029/2006gl026037.

Burbank, D.W., and Fort, M.B. (1985) Bedrock control on glacial limits: Examples from the Ladakh and Zanskar Ranges, north-western Himalaya, India. *Journal of Glaciology*, **31**, 143–149.

Byrne, M. (2009) *Glacier Monitoring in Ladakh and Zanskar, Northwestern India*, Geography Department, University of Montana, Missoula, 124 pp.

CGIAR-CSI (2004) *Void-filled Seamless SRTM Data V1*, International Center for Tropical Agriculture (CIAT). Available at CGIAR-CSI SRTM 90 m Database: *http://srtm.csi.cgiar.org* and *http://www.ambiotek.com/topoview* [Centro Internacional de Agricultura Tropical].

Cogley, J.G., Kargel, J.S., Kaser, G., and Van der Veen, C.J. (2010) Tracking the source of glacier misinformation. *Science*, **327**, 522.

Cuartero, A., Quirós, E., and Felicísimo, A.M. (2005) A study of ASTER DEM accuracies and its dependence of software processing. Paper presented at *Sixth International Conference on Geomorphology, September 7–11, Zaragoza, Spain*.

Dashora, A., Lohani, B., and Malik, J.N. (2007) A repository of Earth resource information: CORONA satellite programme. *Current Science*, **92**(7).

Dimri, A.P., and Kumar, A. (2008) Climatic variability of weather parameters over the western Himalayas: A case study. *Proceedings of the National Snow Science Workshop, January 11–12, Chandigarh*, Snow and Avalanche Study Establishment, Chandigarh, India.

Dobhal, D.P., Gergan, J.T., and Thayyen, R.J. (2008) Mass balance studies of the Dokriani Glacier from 1992 to 2000, Garhwal Himalaya, India. *Bulletin of Glacier Research*, **25**, 9–17.

Dozier, J. (1989a) Remote sensing of snow in the visible and near-infrared wavelengths. In: G. Asrar (Ed.), *Theory and Applications of Optical Remote Sensing*, John Wiley & Sons, New York, pp. 527–547.

Dozier, J. (1989b) Spectral signature of alpine snow cover from the Landsat Thematic Mapper. *Remote Sensing of Environment*, **28**, 9–22.

Driedger, C.L., and Kennard, P.M. (1986) Glacier volume estimation on Cascade volcanoes: An analysis and comparison with other methods. *Annals of Glaciology*, **8**, 59–64.

Dyurgerov, M. (2002 [2005]) *Glacier Mass Balance and Regime: Data of Measurements and Analysis*

(INSTAAR Occasional Paper No. 55, edited by M. Meier and R. Armstrong), Institute of Arctic and Alpine Research, University of Colorado, Boulder.

Dyurgerov, M.B., and Meier, M.F. (2005) *Glaciers and the Changing Earth System: A 2004 Snapshot* (Occasional Paper No. 58), Institute of Arctic and Alpine Research, University of Colorado, Boulder.

Fowler, H.J., and Archer, D.R. (2006) Conflicting signals of climatic change in the Upper Indus Basin. *Journal of Climate*, **19**, 4276–4293.

Fujita, K., and Nuimura, T. (2011) Spatially heterogeneous wastage of Himalayan glaciers. *Proceedings National Academy Sciences U.S.A.*, **108**, 14011–14014.

Fujita, K., Nakawo, M., Fujii, Y., and Paudyal, P. (1997) Changes in glaciers in Hidden Valley, Mukut Himal, Nepal Himalayas, from 1974 to 1994. *Journal of Glaciology*, **43**(145), 583–588.

Fujita, K., Kadota, T., Rana, B., Kayastha, R.B., and Ageta, Y. (2001) Shrinkage of Glacier AX010 in Shorong region, Nepal Himalayas in the 1990s. *Bulletin of Glaciological Research*, **18**, 51–54.

Fujita, K., and Nuimura, T. (2011) Spatially heterogeneous wastage of Himalayan glaciers. *Proceedings National Academy Sciences U.S.A.*, **108**, 14011–14014.

Gadgil, S. (2003) The Indian monsoon and its variability. *Annual Review of Earth and Planetary Sciences*, **31**, 429–467.

Gardelle, J., Berthier, E., and Arnaud, Y. (2012a) Slight mass gain of Karakoram glaciers in the early twenty-first century. *Nature Geoscience*, **5**, 322–325.

Gardelle, J.E., Berthier, E., and Arnaud, Y. (2012b) Impact of resolution and radar penetration on glacier elevation changes computed from DEM differencing. *Journal of Glaciology*, **58**(208), 419–422.

Gautam, R., Hsu, N.C., Lau, K.M., Tsay, S.C., and Kafatos, M. (2009) Enhanced pre-monsoon warming over the Himalayan-Gangetic region from 1979 to 2007. *Geophysical Research Letters*, **36**(L07704), doi: 10.1029/2009GL037641.

Gautam, R., Hsu, N.C., and Lau, K.M. (2010) Premonsoon aerosol characterization and radiative effects over the Indo-Gangetic Plains: Implications for regional climate warming. *Journal of Geophysical Research*, **115**(D17), D17208.

Hall, D.K., Riggs, G.A., and Salomonson, V.V. (1995) Development of methods for mapping global snow cover using Moderate Resolution Imaging Spectroradiometer data. *Remote Sensing of Environment*, **54**, 127–140.

Hambrey, M.J., Quincey, D.J., Glasser, N.F., Reynolds, J.M., Richardson, S.J., and Clemmens, S. (2008) Sedimentological, geomorphological and dynamic context of debris-mantled glaciers, Mount Everest (Sagarmatha) region, Nepal. *Quaternary Science Reviews*, **27**(25/26), 2361–2389.

Hewitt, K. (2005) The Karakoram anomaly? Glacier expansion and the "elevation effect," Karakoram Himalaya. *Mountain Research and Development*, **25**, 332–340.

Hewitt, K. (2011) Glacier change, concentration, and elevation effects in the Karakoram Himalaya, upper Indus Basin. *Mountain Research and Development*, **31**, 188–200.

Higuchi, K., Fushimi, H., Ohata, T., Takenaka, S., Iwata, S., Yokoyama, K., Higuchi, H., Nagoshi, A., and Iozawa, T. (1980) Glacier inventory in the Dudh Kosi region, East Nepal, *World Glacier Inventory* (IAHS-AISH Publication No. 126), International Association of Hydrological Sciences, Rennes, France, pp. 95–103.

Higuchi, K., Ageta, Y., Yasunari, T., and Inoue, J. (1992) Characteristcis of precipitation during the monsoon season in high-mountain areas of the Nepal Himalayas, *Hydrological Aspects of Alpine and High Mountain Areas* (IAHS Publication No. 138), International Association of Hydrological Sciences, Rennes, France, pp. 21–30.

IPCC (2007) *Climate Change 2007: The Physical Science Basis—Summary for Policymakers*, Intergovernmental Panel on Climate Change, Paris, 21 pp.

Iwata, S. (1976) Late Pleistocene and Holocene moraines in the Sagarmatha (Everest) region, Khumbu Himal. *Journal of the Japanese Society of Snow and Ice*, **38**(Special Issue), 109–114.

Iwata, S., Aoki, T., Kadota, T., Seko, K., and Yamaguchi, S. (2000) Morphological evolution of the debris cover on Khumbu Glacier, Nepal, between 1978 and 1995. In: M. Nakawo, C.F. Raymond, and A. Fountain (Eds.), *Debris-covered Glaciers* (IAHS No. 264), International Association of Hydrological Sciences, Rennes, France, pp. 3–11.

Jin, R., Li, X., Che, T., Wu, L., and Mool, P. (2005) Glacier area changes in the Pumqu river basin, Tibetan Plateau, between the 1970s and 2001. *Journal of Glaciology*, **51**(175), 607–610.

Johannesson, T., Raymond, C., and Waddington, E. (1989) Time-scale for adjustment of glaciers to changes in mass balance. *Journal of Glaciology*, **35**(121), 355–369.

Kääb, A. (2005) Combination of SRTM3 and repeat ASTER data for deriving alpine glacier flow velocities in the Bhutan Himalaya. *Remote Sensing of Environment*, **94**(4), 463–474.

Kääb, A., and Vollmer, M. (2000) Surface geometry, thickness changes and flow fields on creeping mountain permafrost: Automatic extraction by digital image analysis. *Permafrost and Periglacial Processes*, **11**, 315–326.

Kääb, A., Huggel, C., Fischer, L., Guex, S., Paul, F., Roer, I., Salzmann, N., Schlaefli, S., Schmutz, K., Schneider, D. et al. (2005) Remote sensing of glacier- and permafrost-related hazards in high mountains: An overview. *Natural Hazards and Earth System Sciences*, **5**(4), 527–554.

Kadota, T., Seko, K., Aoki, T., Iwata, S., and Yamaguchi, S. (2000) Shrinkage of the Khumbu Glacier, east Nepal from 1978 to 1995. In: M. Nakawo, C.F. Raymond, and A. Fountain (Eds.), *Debris-covered Glaciers* (IAHS Publication No. 264), International Association of Hydrological Sciences, Wallingford, U.K., pp. 235–243.

Kamp, U., Byrne, M., and Bolch, T. (2011) Glacier fluctuations between 1975 and 2008 in the Greater Himalaya Range of Zanskar, southern Ladakh. *Journal of Mountain Sciences*, **8**, 374–389.

Kargel, J.S., Abrams, M.J., Bishop, M.P., Bush, A., Hamilton, G., Jiskoot, H., Kääb, A., Kieffer, H.H., Lee, E.M., Paul, F. et al. (2005) Multispectral imaging contributions to global land ice measurements from space. *Remote Sensing of Environment*, **99**(1/2), 187–219.

Kargel, J.S., Cogley, J.G., Leonard, G.J., Haritashya, U., and Byers, A. (2011) Himalayan glaciers: The big picture is a montage. *Proceedings National Academy Sciences U.S.A.*, **108**(36), 14709–14710. Available at *http://www.pnas.org/content/108/36/14709.full*

Karma, Y., Ageta, N., Naito, S., Iwata, S., and Yakubi, H. (2003) Glacier distribution in the Himalayas and glacier shrinkage from 1963 to 1993 in the Bhutan Himalayas. *Bulletin of Glaciological Research*, **20**, 29–40.

Kaser, G., Cogley, J.G., Dyurgerov, M.B., Meier, M.F., and Ohmura, A. (2006) Mass balance of glaciers and ice caps: Consensus estimates for 1961–2004. *Geophysical Research Letters*, **33**(19), doi: 10.1029/2006GL027511.

Kaser, G., Großhauser, M., and Marzeion, B. (2010) Contribution potential of glaciers to water availability in different climate regimes. *Proceedings National Academy Sciences U.S.A.*, November 23, **107**(47), 20223–20227.

Kayastha, R.B., Takeuchi, Y., Nakawo, M., and Ageta, Y. (2000) Practical prediction of ice melting beneath various thickness of debris cover on Khumbu Glacier, Nepal, using a positive degree-day factor. In: C.F. Raymond, M. Nakawo, and A. Fountain (Eds.), *Debris-covered Glaciers* (IAHS Publication No. 264), International Association of Hydrological Sciences, Wallingford, U.K., pp. 71–81.

Keller, F. (1992) Automated mapping of mountain permafrost using the program PERMAKART within the Geographical Information System ARC/INFO. *Permafrost and Periglacial Processes*, **3**(2), 133–138.

King, M.D., Closs, J., Greenstone, R., Wharton, S., and Myers, M. (2003) *EOS Data Products Handbook*, Vol. 1, NASA Goddard Space Flight Center, Greenbelt, MD.

Krishna, A.P. (2005) Snow and glacier cover assessment in the high mountains of Sikkim Himalaya. *Hydrological Processes*, **19**(12), 2375–2383.

Kulkarni, A.V. (1992) Glacier inventory in the Himalaya, *Natural Resources Management: A New Perspective*, National Natural Resource Management System, Department of Space, Bangalore, India, pp. 474–478.

Kulkarni, A.V., and Bahuguna, I.M. (2002) Glacial retreat in the Baspa basin, Himalaya, monitored with satellite stereo data. *Journal of Glaciology*, **48**(160), 171–172.

Kulkarni, A.V., and Buch, A.M. (1991) *Glacier Atlas of Indian Himalaya* (SAC/RSA/RSAG-MWRD/SN/05/91), Divecha Center for Climate Change, Indian Institute of Science, Bangalore, India, 52 pp.

Kulkarni, A.V., Rathore, B.P., Mahajan, S., and Mathur, P. (2005) Alarming retreat of Parbati glacier, Beas basin, Himachal Pradesh. *Current Science*, **88**(11), 1844–1850.

Kulkarni, A.V., Bahuguna, I.M., Rathore, B.P., Singh, S.K., Randhawa, S.S., Sood, R.K., and Dhar, S. (2007) Glacial retreat in Himalaya using Indian remote sensing satellite data. *Current Science*, **92**(1), 69–74.

Lau, W.K.M., Kim, M.-K., Kim, K-M., and Lee W.-S. (2010) Enhanced surface warming and accelerated snow melt in the Himalayas and Tibetan Plateau induced by absorbing aerosols. *Environmental Research Letters*, **5**(2), doi: 10.1088/1748-9326/5/2/025204.

Liu, C., and Sharma, C.K. (1988) *Report on First Expedition to Glaciers in the Pumqu (Arun) and Poiqu (Bhote-Sun Kosi) River Basins, Xizang (Tibet), China*, Science Press, Beijing, China, 192 pp.

Maisch, M. (1992) Die Gletscher Graubündens: Rekonstruktionen und Auswertung der Gletscher und deren Veränderungen seit dem Hochstand von 1850 im Gebiet der östlichen Schweizer Alpen. *Physical Geography*, **33A/B**(324), 168 [in German].

Manley, W.F. (2008) Geospatial inventory and analysis of glaciers: A case study for the eastern Alaska Range. In: R.S. Williams Jr., and J.G. Ferrigno (Eds.), *Satellite Image Atlas of Glaciers of the World* (USGS Professional Paper 1386-K), U.S. Geological Survey, Reston, VA.

Mason, K. (1954) *Abode of Snow: A History of Himalayan Exploration and Mountaineering*, Dutton, New York.

Mayewski, P.A., and Jeschke, P.A. (1979) Himalayan and trans-Himalayan glacier fluctuations since AD 1812. *Arctic, Antarctic, and Alpine Research*, **11**(3), 267–287.

Mayewski, P.A., Pregent, G.P., Jeschke, P.A., and Ahmad, N. (1980) Himalayan and trans-Himalayan glacier fluctuations and the South Asian monsoon record. *Arctic and Alpine Research*, **12**(2), 171–182.

Ming, J., Du, Z., Xiao, C., Xu, X., and Zhang, D. (2012) Darkening of the mid-Himalaya glaciers since 2000 and the potential causes. *Environmental Research Letters*, **7**, 014021.

Mool, P.K., Bajracharya, S.R., and Joshi, S.P. (2002) *Inventory of Glaciers, Glacial Lakes and Glacial Lake Outburst Floods Monitoring and Early Warning Systems in the Hindu-Kush Himalayan region: Nepal*, International Center for Integrated Mountain Development, Kathmandu, Nepal.

Müller, F. (1970) Inventory of glaciers in the Mount Everest region, *Perennial Ice and Snow Masses*, UNESCO, Paris, France/International Association of Hydrological Sciences, Rennes, France, pp. 47–53.

Nainwal, H.C., Negi, B.D.S., Chaudhary, M., Sajwan, K.S., and Gaurav, A. (2008) Temporal changes in rate of recession: Evidences from Satopanth and Bhagirath Kharak glaciers, Uttarakhand, using Total Station Survey. *Current Science*, **94**(5), 653–660.

Nakawo, M., and Rana, B. (1999) Estimate of ablation rate of glacier ice under a supraglacial debris layer. *Geografiska Annaler: Series A, Physical Geography*, **81**(4), 695–701.

Nakawo, M., Morohoshi, T., and Uehara, S. (1993) Satellite data utilization for estimating ablation of debris covered glaciers. In: G.J. Young (Ed.), *Snow and Glacier Hydrology: Proceedings of the International Symposium, Kathmandu, Nepal, November 16-21, 1992* (IAHS-AISH Publication No. 218), International Association of Hydrological Sciences, Rennes, France pp. 75–83.

Nuimura, T., Fujita, K., Yamaguchi, S., and Sharma, R.R. (2012) Elevation changes of glaciers revealed by multitemporal digital elevation models calibrated by GPS survey in the Khumbu region, Nepal Himalaya, 1992–2008. *Journal of Glaciology*, **58**(210), 648–656.

Nuth, C., and Kääb, A. (2011) Co-registration and bias corrections of satellite elevation data sets for quantifying glacier thickness change. *The Cryosphere*, **5**, 271–290.

Paul, F., Kääb, A., Maisch, M., Kellenberger, T., and Haeberli, W. (2002) The new remote-sensing-derived Swiss glacier inventory, I: Methods. *Annals of Glaciology*, **34**, 355–361.

Quincey, D.J., Luckman, A., and Benn, D. (2009) Quantification of Everest region glacier velocities between 1992 and 2002, using satellite radar interferometry and feature tracking. *Journal of Glaciology*, **55**, 596–606.

Racoviteanu, A., and Williams, M.W. (2012) Decision tree amd texture analysis for mapping debris-covered glaciers in the Kangchenjunga area, Eastern Himalaya. *Remote Sensing*, **4**(10), 3078–3109..

Racoviteanu, A., Arnaud, Y., and Williams, M. (2008) Decadal changes in glacier parameters in Cordillera Blanca, Peru derived from remote sensing. *Journal of Glaciology*, **54**(186), 499–510.

Racoviteanu, A., Paul, F., Raup, B., Khalsa, S.J.S., and Armstrong, R. (2009) Challenges and recommendations in mapping of glacier parameters from space: Results of the 2008 Global Land Ice Measurements from Space (GLIMS) Workshop, Boulder, Colorado, USA. *Annals of Glaciology*, **50**(53), 53–69.

Raina, V.K. (2009) *Himalayan Glaciers: A State-of-Art Review of Glacial Studies, Glacial Retreat and Climate Change* (Discussion Paper), Ministry of Environment and Forests, Government of India, New Delhi, 56 pp. Available at *http://moef.nic.in/downloads/public information/MoEF%20Discussion%20Pape%20_him.pdf*

Raina, V.K., and Srivastava, D. (2008) *Glacier Atlas of India*, Geological Society of India, Bangalore, 315 pp.

Ren, D., Karoly, D.J., and Leslie, L.M. (2007) Temperate mountain glacier-melting rates for the period 2001–30: Estimates from three coupled GCM simulations for the Greater Himalayas. *Journal of Applied Meteorology and Climatology*, **46**(6), 890–899.

Richardson, S.D., and Reynolds, J.M. (2000) An overview of glacial hazards in the Himalayas. *Quaternary International*, **65**(6), 31–47.

Sah, M., Philip, G., Mool, P.K., Bajracharya, S., and Shrestha, B. (2005) *Uttaranchal Himalaya India: Inventory of Glaciers and Glacial Lakes and the Identification of Potential Glacial Lake Outburst Floods (GLOFs) Affected by Global Warming in the Mountains of Himalayan Region* (report in CD-ROM format), International Center for Integrated Mountain Development, Kathmandu, Nepal, 176 pp.

Sangewar, C.V., and Shukla, S.P. (Eds.) (1999) *Inventory of the Himalayan Glaciers: A Contribution to the International Hydrological Programme* (Special Publication No. 34: Updated Edition), Geological Survey of India, Bangalore.

Sangewar, C.V. and Shukla, S.P. (Eds.) (2009) *Inventory of Himalayan Glaciers: A Contribution to the International Hydrological Programme* (GSI Special Publication 34, an updated edition), Geological Survey of India, Calcutta, India.

Salerno, F., Buraschi, E., Bruccoleri, G., Tartari G., and Smiraglia, C. (2008) Glacier surface-area changes in Sagarmatha national park, Nepal, in the second half of the 20th century, by comparison of historical maps. *Journal of Glaciology*, **54**(187), 738–752.

Scherler, D., Bookhagen, B., and Strecker, M.R. (2011) Spatially variable response of Himalayan glaciers to climate change affected by debris cover. *Nature Geoscience*, **4**, 156–159, doi: 10.1038/ngeo1068.

Schmidt, S., and Nusser, M. (2009) Fluctuations of Raikot Glacier during the past 70 years: A case study from the Nanga Parbat massif, northern Pakistan. *Journal of Glaciology*, **55**(194), 949–959.

Shanker, R. (1999). Glaciological studies in India: Contributions from Geological Survey of India. Paper presented at *Symposium on Snow, Ice and Glaciers: A Himalayan Perspective, Lucknow, March 9–11, 1999*.

Shekhar, M.S., Chand, H., Kumar, S., Srinivasan, K., and Ganju, A. (2010) Climate-change studies in the

western Himalaya. *Annals of Glaciology*, **51**(54), 105–112.

Shen, Y. (2004) *An Overview of Glaciers: Retreating Glaciers and Their Impact in the Tibetan Plateau*, Cold and Arid Regions Environmental and Engineering Research Institute (CAREERI), Chinese Academy of Sciences (CAS), Lanzhou, China, 42 pp.

Shrestha, A.B., Wake, C.P., Mayewski, P.A., and Dibb, J.E. (1999) Maximum temperature trends in the Himalaya and its vicinity: An analysis based on temperature records from Nepal for the period 1971–94. *Bulletin of the American Meteorological Society*, **12**, 2775–2786.

Shrestha, M.L. (2000) Interannual variation of summer monsoon rainfall over Nepal and its relation to the Southern Oscillation index. *Meteorology and Atmospheric Physics*, **75**, 21–28.

Singh, P. (2000) Degree-day factors for snow and ice for Dokriani Glacier, Garhwal Himalayas. *Journal of Hydrology*, **235**(1/2), 1–11.

Singh, P., Kumar, N., Ramasastri, K.S., and Singh, Y. (2000) Influence of a fine debris layer on the melting of snow and ice on a Himalayan glacier. In: M. Nakawo, C.F. Raymond, and A. Fountain (Eds.), *Debris-covered Glaciers* (IAHS Publication No. 264), International Association of Hydrological Sciences, Wallingford, U.K., pp. 63–69.

Srikantia, S.V. (2000) Restriction on maps: A denial of valid geographic information. *Current Science*, **79**(4), 484–488.

Srivastava, D. (2004) *Recession of Gangotri Glacier* (Geological Survey of India Special Publication No. 80), Geological Survey of India, Bangalore, pp. 21–32.

Stokes, C.R., Popovnin, V., Aleynikov, A., Gurney, S.D., and Shahgedanova, M. (2007) Recent glacier retreat in the Caucasus Mts, Russia, and associated increase in supraglacial debris cover and supra/proglacial lake development. *Annals of Glaciology*, **46**, 195–203.

Survey of India (2005) National Map Policy. Available at *http://www.surveyofindia.gov.in/tenders/nationalmappolicy/nationalmappolicy.pdf* [accessed October 24, 2010].

Takeuchi, Y., Kayastha, R.B., and Nakawo, M. (2000) Characteristics of ablation and heat balance in debris-free and debris-covered areas on Khumbu Glacier, Nepal Himalayas, in the pre-monsoon season. In: M. Nakawo, C.F. Raymond, and A. Fountain (Eds.), *Debris-covered Glaciers* (IAHS Publication No. 264), International Association of Hydrological Sciences, Wallingford, U.K., pp. 53–61.

Tartari, G., Verza, G.P., and Bertolami, L. (1998) Meteorological data at the Pyramid Observatory Laboratory (Khumbu Valley, Sagarmatha National Park, Nepal). *Memorie dell'Istituto Italiano di Idrobiologia*, **57**, 23–40.

Toutin, T. (2008) ASTER DEMs for geomatic and geoscientific applications: A review. *International Journal of Remote Sensing*, **29**(7), 1855–1875.

USGS-EROS (1996) USGS Declassified Imagery-1. Available at *http://eros.usgs.gov/#/Guides/disp1* [retrieved August 15, 2011].

Vohra, C.P. (1980) *Some Problems of Glacier Inventory in the Himalaya* (IAHS Publication No. 126), International Association of Hydrological Sciences, Rennes, France, pp. 67–74.

Wagnon, P., Linda, A., Arnaud, Y., Kumar, R., Sharma, P., Vincent, C., Pottakkal, J.G., Berthier, E., Ramanathan, A., Hasnain, S.I. et al. (2007) Four years of mass balance on Chhota Shigri Glacier, Himachal Pradesh, India, a new benchmark glacier in the western Himalaya. *Journal of Glaciology*, **53**(183), 603–611.

Watanabe, T., Kameyama, S., and Sato, T. (1995) Imja Glacier dead-ice melt rates and changes in a supraglacial lake, 1989–1994, Khumbu Himal, Nepal: Danger of lake drainage. *Mountain Research and Development*, **15**(4), 293–300.

WWF (2005) *An Overview of Glaciers, Glacier Retreat, and Subsequent Impacts in Nepal, India and China* (WWF Nepal Program), World Wildlife Fund, Washington, D.C., 79 pp.

Yamada, T., Shiraiwa, T., Iida, H., Kadota, T., Watanabe, T., Rana, B., Ageta, Y., and Fushimi, H. (1992) Fluctuations of the glaciers from the 1970s to 1989 in the Khumbu, Shorong and Langtang regions, Nepal Himalayas. *Bulletin of Glacier Research*, **10**, 11–19.

Yanai, M., Li, C., and Song, Z. (1992) Seasonal heating of the Tibetan plateau and its effect on the evolution of the Asian summer monsoon. *Journal of Meteorological Society of Japan*, **70**, 319–351.

Yao, T., Thompson, L., Yang, W., Yu, W., Gao, Y., Guo, X., Yang, X., Duan, K., Zhao, H., Xu, B. et al. (2012) Different glacier status with atmospheric circulations in Tibetan Plateau and surroundings. *Nature Climate Change*, **2**(8), 663–667, doi: 10.1038/nclimate1580.

Zgorzelski, M. (2006) Ladakh and Zanskar. *Miscellanea Geographica*, **12**, 13–24.